# Carbonyl Reductase - Like 20β-Hydroxysteroid Dehydrogenases in the Ovarian Follicle of a Teleost Fish, the Rainbow Trout (*Oncorhynchus mykiss*): Their Structures and Reproductive Functions in Oocyte Maturation

**By**

**Guijin GUAN**

***PhD in Science***

**Department of Molelucar Biomechanics**

**School of Life Science**

**The Graduate University for Advanced Studies**

**1999**

## CONTENTS

# ABSTRACT

Meiotic maturation of the oocyte (oocyte maturation) occurs prior to ovulation and is a prerequisite for successful fertilization. Oocyte maturation has been studied in various animal species, but its endocrine regulation has been investigated most extensively in fishes. It is now established that three major mediators, gonadotropin (GTH), in particular luteinizing hormone (LH, GTH-II in fish), maturation-inducing hormone (MIH), and maturation-promoting factor (MPF) are involved in the induction of oocyte maturation. 17α,20β-dihydroxy-4-pregnen-3-one (17α,20β-DP) was identified as the MIH of several teleost fishes including salmonid fishes. The interaction of two ovarian follicle cell layers, the thecal and granulosa cell layers, is required for the synthesis of 17α,20β-DP. The thecal layer produces 17α-hydroxyprogesterone (17α-HP) that is converted to 17α,20β-DP in granulosa cells by the action of 20β-hydroxysteroid dehydrogenase (20β-HSD). In this study, as a first step to investigate the molecular mechanism of GTH-regulated MIH production by fish ovarian follicles, 20β-HSD cDNAs were cloned from postvitellogenic ovarian follicles of a salmonid fish, the rainbow trout, *Oncorhynchus mykiss* (Chapter I). A series of studies employing site-directed mutagenesis were conducted to characterize the coenzyme NADPH-binding of rainbow trout 20β-HSD (Chapter II). Finally, dynamic changes in mRNA levels of 20β-HSD in ovarian follicles during oocyte growth and maturation were determined and compared with those of 3β-hydroxysteroid dehydrogenase (3β-HSD) and cytochrome P450 aromatase (P450arom) with a particular emphasis on GTH regulation of 20β-HSD gene expression in ovarian granulosa cells (Chapter III).

Two closely related 20β-HSD cDNAs were cloned from rainbow trout ovarian follicles. Both cDNAs belong to the short-chain dehydrogenase/reductase (SDR) family, with approximately 60% homology to mammalian carbonyl reductases (CRs) and termed rainbow trout CR/20β-HSD cDNA type A and type B. Type A and type B share high homology of 99% at the nucleotide level and 98.7% at the amino acid level within their open reading frames. Using the type B cDNA fragment, two clones, termed CR/20β-HSD genes I and II, were obtained from the λDASH genomic library of rainbow trout. The sequences of the cDNAs deduced from CR/20β-HSD genes I and II matched with CR/20β-HSD cDNA type A and type B, respectively. Genomic DNA analysis showed that the two

CR/20β-HSD cDNAs are derived from two different genes. Both rainbow trout CR/20β-HSD genes consist of four exons. The structural organization of the genes is very similar, with the introns interrupting the genes at the same locations. Genes I and II sequences share 53% identity in the 5' upstream regions up to –700 bp from the initiation site. Comparison of the amino acid sequences of rainbow trout CR/20β-HSD with mammalian CRs reveals that the Rossmann fold, GlyXXXGlyXGly, which is the co-factor binding site, is well conserved. Although the functional significance of the two genes remains unresolved, these results clearly demonstrate the presence of two distinct CR/20β-HSD transcripts in the trout ovary.

Recombinant CR/20β-HSD proteins produced in *E. coli* were incubated with [$^3$H]-17α-HP in the presence of NADPH and resulting steroids were separated by thin layer chromatograpy. A band which comigrated with authentic 17α,20β-DP was obtained from incubations of CR/20β-HSD type A, indicating that CR/20β-HSD type A cDNA encodes a protein with 20β-HSD activity. Recombinant CR/20β-HSD type A also catalyzed the reduction of a number of characteristic substrates of CR with efficient catalyzation of the reduction of quinones, or menadione, whereas prostaglandins and steroids including 17α-HP were reduced at lower rates. Recombinant protein derived from CR/20β-HSD type B cDNA did not recognize any of these substrates.

Northern blot analysis demonstrated that trout CR/20β-HSDs are expressed in various tissues, of greatest abundance in liver and gill, followed by brain, ovary and testis, adipose tissue, and kidney. Results of RT-PCR employing primers specific for CR/20β-HSD cDNA A and B were consistent with that of Northern blot, showing that CR20β-HSD cDNAs type A and type B were expressed in most tissues, but only the expression of CR/20β-HSD type A could be detected in liver.

As described above, trout CR/20β-HSD type B does not possess either CR or 20β-HSD activity. Among their three distinct amino acids, Ile15 in trout CR/20β-HSD type A was found to be well converted among many CRs. It is substituted to Thr in CR/20β-HSD type B. To test if this mutation is responsible for abolishing the stability of enzyme and co-enzyme complex, several mutations of CR/20β-HSD were created by site-directed mutagenesis and the enzyme activity of their recombinants expressed in *E. coli* were determined. Mutation of I15T in type A abolished enzyme activity with different

substrates, and mutation of T15I in type B resulted in the acquisition of enzyme activity. Furthermore, by fluorescence titration assay, it was found that I15 is crucial in permitting the formation of the CR/20β-HSD – co-enzyme (NADPH) complex. Mutation of A/I15T abolished the ability of the trout CR/20β-HSD type A enzyme to bind with NADPH and further caused the enzyme to lose its activity. Taken together, these data provide evidence that Ile is critical in the GlyXXXGlyXGly co-factor binding structure.

Northern blotting revealed that 3β-HSD mRNA levels steadily increased during the vitellogenic stage, was further enhanced at oocyte maturation stage, and kept in high levels in postovulatory follicles. P450arom mRNA levels were high during active vitellogenesis, but rapidly decreased before oocyte maturation with undetectable levels at oocyte maturation and in postovulatory follicles. In contrast to the change in P450arom gene expression, CR/20β-HSD mRNA levels were low in follicles during active vitellogenesis, but markedly increased during oocyte maturation and remained high during the postovulatory stage.

A major finding in this study is that CR/20β-HSD gene expression was markedly enhanced when granulosa cells isolated from postvitellogenic follicles were incubated with GTH. Furthermore, there was an increase in CR/20β-HSD enzyme content after GTH stimulation. It is also of importance to note that CR/20β-HSD type A gene, but not type B gene, is inducible in granulosa cells by GTH stimulation. Since CR/20β-HSD type A exhibits 20β-HSD activity, the enhanced expression of CR/20β-HSD type A gene increases the conversion of 17α-HP to 17α,20β-DP. These data provide information on dynamic molecular changes during oocyte growth and maturation, and also demonstrate that the expression of 20β-HSD and 3β-HSD gene is controlled by GTH. The effects of GTH on the promoter regions of CR/20β-HSD genes will provide further understanding of steroid and protein hormone modulation of steroidogenic enzymes.

# CHAPTER I

## Cloning and expression of two carbonyl reductase - like 20β-hydroxysteroid dehydrogenase cDNAs in ovarian follicles of rainbow trout

# INTRODUCTION

Meiotic maturation of the oocyte (oocyte maturation) is a crucial step in the development of a fertilizable gamete. In teleosts, oocyte maturation is regulated by an oocyte follicle-derived steroidal mediator, maturation-inducing hormone (MIH), under the control of gonadotropin (GTH). It is now apparent that fish GTHs, GTH-I and GTH-II, are chemically and biologically similar to tetrapod follicle-stimulating hormone (FSH) and luteinizing hormone (LH), respectively (Kawauchi *et al.*, 1989; Swanson, 1991). Like FSH, GTH-I is secreted during the period of gonadal growth (vitellogenesis and spermatogenesis) and functions to stimulate gonadal growth and steroidogenesis at this stage. Like LH, GTH-II was reported to increase during the period of final oocyte maturation to alter steroidogenesis to promote oocyte and sperm maturation (Nagahama, 1994). In this thesis, the term GTH refers to GTH-II preparations (LH-like GTH), some of which may be contaminated by GTH-I.

It is now well established that like amphibians, oocyte maturation in fish is regulated by three major mediators, GTH, MIH, and maturation-promoting factor (MPF), that function sequentially at the level of the ovarian follicle cells, the oocyte surface, and oocyte cytoplasm (Wasserman and Smith, 1978; Masui and Clarke, 1979; Nagahama *et al.*, 1995; Yamashita *et al.*, 1995) (Fig. 1). 17α,20β-dihydroxy-4-pregnen-3-one (17α,20β-DP) has been identified as the natural MIH in salmonid fish (Nagahama and Adachi, 1985; Nagahama, 1997), and a two cell-type model has been proposed for the production of 17α,20β-DP by salmonid ovarian follicles (Young *et al.*, 1986). In this model (Fig. 2), GTH stimulates the thecal layer to produce 17α-hydroxyprogesterone (17α-HP), and also acts on the granulosa cell layer to rapidly enhance 20β-hydroxysteroid dehydrogenase (20β-HSD) activity, which converts 17α-HP to 17α,20β-DP. It has been suggested that GTH causes the *de novo* synthesis of 20β-HSD by a mechanism dependent on RNA synthesis (Nagahama *et al.*, 1985), via an adenylate cyclase-cAMP pathway (Kanamori and Nagahama, 1988). Thus, 20β-HSD is the key enzyme involved in the production of MIH, and GTH-induced 20β-HSD synthesis in salmonid granulosa cells is a good model for the study of cell-specific regulation of gene expression in eukaryotic cells. However, the

molecular events underlying the GTH-regulated 20β-HSD synthesis have not yet been elucidated because the cDNA(s) encoding salmonid 20β-HSD has not been cloned.

Tanaka and others in our laboratory have reported the cloning of 20β-HSD cDNA from neonatal pig testes (Tanaka *et al.*, 1992). Interestingly, pig 20β-HSD shows high similarity to carbonyl reductase (CR) from human (Wermuth *et al.*, 1988) and rat (Wermuth *et al.*, 1995; Aoki *et al.*, 1997), and pig 20β-HSD has a very strong CR activity (Nakajin *et al.*, 1997), suggesting that pig 20β-HSD is identical to pig CR. This was named CR/20β-HSD. CR/20β-HSDs belong to the short-chain steroid dehydrogenase/ reductase (SDR) family (Jornvall *et al.*, 1995), and catalyze the NADPH-dependent reduction of a large number of biological and pharmacological substrates. However, in mammals, little is known about the physiological function of CR/20β-HSD, especially in relation to gonadal steroidogenesis. A recent report shows that expression of one of two genes in rat ovary which encode proteins with high similarity to CR/20β-HSD is under the control of GTH (Aoki *et al.*, 1997), suggesting that CR/20β-HSD plays an important role in GTH-regulated ovarian function.

In the present study, as a first step to investigate the molecular mechanism of GTH-regulated MIH production in salmonids, I cloned CR/20β-HSD cDNAs from rainbow trout ovarian follicles and analyzed the enzymatic activity of the proteins they encode. In addition, the tissue distribution of CR/20β-HSD mRNAs was also determined by Northern blot and RT-PCR analyses.

# MATERIALS AND METHODS

### *cDNA and genomic cloning*

A CR/20β-HSD cDNA fragment from ayu (*Plecoglossus altivelis*) ovary (Tanaka *et al.*, 1996) was used as a probe to screen a λgt 10 ovarian follicle cDNA library prepared from rainbow trout (*Oncorhynchus mykiss*) ovary containing fully-grown follicles just prior to maturation. A genomic λDASH rainbow trout library (gift from Dr. Thomas Chen, University of Connecticut) was screened using a rainbow trout CR/20β-HSD cDNA clone (clone B, see below) obtained from the rainbow trout cDNA library as a probe. Inserts of both cDNA and genomic clones were further subcloned into pBluescript SK$^-$ vectors and sequenced with an ABI PRISM$^{TM}$ 377 DNA Sequencer. All the sequences were confirmed by bi-directional determination and deposited into Genbank (accession number AF 100930-33). Overlapping sequences were assembled using the Auto Assembler (ABI PRISM) software package. Database searches were performed using BLAST. Homology analysis of nucleotide sequences and deduced protein alignment were performed with DNASIS and Mac Vector sequence analysis software (Oxford).

### *5' RACE*

The 5' end sequence of one of the rainbow trout CR/20β-HSD cDNAs (clone A) was determined by 5' Rapid Amplification of cDNA End system (Gibco BRL). The nested gene-specific primer (primer G3A, 5' CATTCACCACTCTGGCATTTGG 3') was designed to anneal to 511nt - 532nt of the rainbow trout CR/20β-HSD cDNA A. Three 5' RACE products of different sizes were cloned into TA-cloning vector, pGEM T-easy (Gibco BRL), and subsequently characterized.

### *In vitro expression of rainbow trout CR/20β-HSD cDNA A and B in E. coli*

Two primers were designed to introduce an *Nde*I site at the 5' end and a *Bam*HI site at the 3' end of the open reading frame (ORF) of the two rainbow trout CR/20β-HSD cDNAs (clone A and B). The PCR amplified products were inserted into a bacterial expression vector (pET21b$^+$) at the *Nde*I and *Bam*HI sites, and introduced into *E. coli* BL21 strain. The expression constructs were verified by nucleotide sequence analysis.

Fifty-ml cultures were harvested and 1-ml homogenized lysates were recovered. After 100,000 rpm centrifugation, the supernatants were collected and used to measure 20β-HSD activity by the conversion of 17α-HP into 17α, 20β-DP. After incubation at 28°C with [$^3$H]-17α-HP (1.48-2.22 TBq/mmol; NEN), products were separated on a high performance TLC plate (Merck) in a benzene/acetone (4 : 1) solvent system, which was then exposed to Hyperfilm (Amersham). A spot with the same mobility as cold standard 17α,20β-DP was extracted with ethanol, and further identified by recrystallization according to the mothod of Axelrod *et al.* (1965).

Carbonyl reductase activity was determined using the method described by Wermuth et al. (1988). Clear lysates were harvested from 200-ml cultures of BL21 transformed with expression constructs, as described above. The lysates were purified by fast protein liquid chromatography (FPLC) through DEAE Sepharose fast flow (Pharmacia). The absorbed proteins were eluted using a linear gradient of 0 to 0.4 M NaCl in 20 mM Tris-HCl/1 mM EDTA solution (pH 8.0). Carbonyl reductase activity was measured by the decrease in absorbance at 340 nm in the presence of 0.08 mM NADPH in Tris-buffer (pH 8.0) at 25°C.

***Northern analysis***

Total RNAs were prepared from adipose tissue, brain, gill, head kidney, posterior kidney, liver, heart, muscle, testis and ovary of rainbow trout in the vitellogenic stage using ISOGEN (Nippon Gene), and poly (A)+ RNAs were purified using Oligotex-DT30 (Takara). The poly(A)+ RNAs (2.5 μg) were separated on a formaldehyde-agarose gel, and transferred onto a nylon membrane (Hybond$^{TM}$-N+, Amersham). The membrane was hybridized with the 5' end of the cDNA A fragment, labeled with [$^{32}$P]-dCTP by PCR amplification using:

primer AS (5' CAACTCTGGTTTAAATAATGTAATTAGCTGTGCTGGTGA 3')

and primer G3A (5' CATTCACCACTCTGGCATTTGG 3'). After stripping hybridized probe from the membrane, a control rehybridization was performed with a rainbow trout β-actin cDNA probe. The data were quantified by an image analyzer (BAS 2000 Imager, Fuji).

***Reverse-transcription and polymerase chain reaction (RT- PCR)***

One microgram of total RNA extracted from each tissue was reverse-transcribed to first-strand cDNA using a cDNA Synthesis Kit (Takara). A portion (1/25) of the reaction mixture was subjected to PCR amplification. Forward primer specific for CR/20β-HSD cDNA A was: 5'-TCACCAGCACAGCTAATTACATTATTTAAACCAGAGTTG(35-73) and the specific primer for CR/20β-HSD cDNA B was 5'-CTACAACCACAGTGCGGT (22-39). The reverse primer was the same for both CR/20β-HSD cDNAs A and B (primer G3A 5'-CATTCACCACTCTGGCATTTGG). PCR reaction was performed at 94°C for 1 min, 62°C for 1 min and 72°C for 1 min for 30 cycles using a Perkin-Elmer 480 thermal cycler.

# RESULTS

***Isolation of two CR/20β-HSD genes (clone A and clone B) from rainbow trout ovarian follicles***

The ayu CR/20β-HSD cDNA clone was used as a probe to screen the rainbow trout ovarian follicle cDNA library. Thirteen positive clones were recovered from screening of two million λgt10 phage plaques. The phage clones containing the larger cDNA inserts were subcloned into pBluescript SK⁻ and further characterized. Two cDNAs whose sequences exhibited high homology to ayu (84%) and pig (61%) CR/20β-HSDs were obtained and termed rainbow trout CR/20β-HSD cDNA type A and B (Fig. 3). Type B cDNA contains an open reading frame of 828 nucleotides, with 114 nucleotides in the 5' noncoding region, and 271 nucleotides in the 3' noncoding region including one polyadenylation site. The predicted molecular weight of the deduced protein encoded by the ORF is 30.1 kDa, and the predicted isoelectric point (pI) is 7.58 with DNASIS. Type A contains an incomplete ORF missing the 5'-end with 324 nucleotides in the 3' noncoding region including a poly(A) signal. Since the 5'-end of type A was truncated, 5' RACE was carried out to fill the 5' end of the clone A. Three amplified products from 5' RACE of different sizes were subcloned into TA cloning vector and sequenced. All overlapped and the largest fragment was added on the 5' end of type A. Like type B, type A cDNA also contains an ORF of 828 nucleotides and encodes a 276 amino acids product with a pI of 7.89. Type A and type B shared high homology of 99% at the nucleotide level and 98.7% at the amino acid level within their ORFs. The homology of the 5' noncoding regions is 77%, while that of the 3' noncoding region is 91%.

Using the type B cDNA fragment as a probe, we screened the λDASH genomic library of rainbow trout. Four positive clones were isolated from one million phage plaques. Two clones, termed CR/20β-HSD genes I and II, showed different restriction patterns and were further sequenced. The exon and intron organization of the genes was determined by comparing cDNA sequences. The sequence of the cDNA deduced from CR/20β-HSD gene I matched perfectly with CR/20β-HSD cDNA type A. cDNA sequence deduced from CR/20β-HSD gene II matched with CR/20β-HSD cDNA type B except for two nucleotides. Structures of the genes are depicted in Fig. 4, and characteristics of the

exons and introns are listed in Table 1. Both rainbow trout CR/20β-HSD genes consist of four exons. The structural organization of the genes is very similar, with the introns interrupting the genes at the same locations. However, some of the introns are of different sizes. The sequence homology between the rainbow trout CR/20β-HSD genes I and II are shown in Table 1. There is a putative TATA box in the upstream region of both rainbow trout CR/20β-HSD I and II, but sequence homology decreases upstream from the TATA box. The sequences of genes I and II share 53% identity in the 5' upstream regions up to -700 bp from the initiation site (Fig. 5).

Comparison of the amino acid sequences of rainbow trout CR/20β-HSDs with several mammalian carbonyl reductases, members of the SDR family, is shown in Fig. 6. The Rossmann fold, GlyXXXGlyXGly, which is the co-factor binding site, is well conserved among these enzymes, as is the TyrXXXLys motif which is critical to the catalytic activity (Jornvall *et al.*, 1995).

***Enzymatic characterization of recombinant CR/20β-HSD proteins***

Both ORFs of cDNA clone A and B were inserted into the expression vector pET21b+ to yield pET21b+rcA and pET21b+rcB. Sequence analysis of expression constructs had confirmed that all were identical to the original cDNAs. The expression constructs were introduced into BL21 strain by heat shock. Protein expressed from pET21b+rcA and pET21b+rcB were confirmed to be 30 kDa by SDS-PAGE electrophoresis, and the N-terminal amino acid sequences were confirmed by an amino acid analyser (ABI 494).

Products from pET21b+rcA, pET21b+rcB, or pET21b+ only, were incubated with [$^3$H]-17α-HP in the presence of NADPH and resulting steroids were separated by TLC (Fig. 7). A band which comigrated with authentic 17α,20β-DP was obtained from incubations of pET21b+rcA lysates with [$^3$H]-17α-HP. This band was extracted and recrystallized. The extraction ratio from three crystallizations in different solvent systems was the same as that for cold 17α,20β-DP (Table 2), indicating that CR/20β-HSD type A cDNA encodes a protein with 20β-HSD activity. Lysates from pET21b+rcB or pET21b+ did not convert 17α-HP to 17α,20β-DP.

Recombinant enzyme from pET21b+rcA also catalyzed the reduction of a number of characteristic substrates of CR (Table 3). Like human CR and pig 20β-HSD, it efficiently catalyzed the reduction of quinones (4-nitrobenzaldehyde), or menadione, whereas prostaglandins and steroids including 17α-HP were reduced at lower rates. The CR/20β-HSD type A recombinant enzyme also reduced both 5α- and 5β-dihydrotestosterone. Recombinant protein derived from pET21b+rc B did not recognize any of these substrates.

***Expression of CR/20β-HSDs in various tissues of rainbow trout***

Since the nucleotide sequences of CR/20β-HSD cDNAs A and B are very similar, their mRNAs are difficult to distinguish from each other by Northern hybridization. In this study, the CR/20β-HSD cDNA A was used as the probe to investigate the tissue distribution of CR/20β-HSD mRNAs in rainbow trout. The result of Northern blot analysis is shown in Fig. 8. A single band of 1.34 kb was detected in most of tissues examined, of greatest abundance in liver and gill, followed by brain, ovary and testis, adipose tissue, head kidney and posterior kidney. A very weak hybridization signal was obtained using muscle RNA. Results of RT-PCR employing primers specific for CR/20β-HSD cDNAs A and B was consistent with that of Northern blot, showing that CR/20β-HSD cDNA A and CR/20β-HSD cDNA B were expressed in most tissues (Fig. 9), but only the expression of CR/20β-HSD A could be detected in liver. No signal could be detected in heart either by Northern analysis or by RT PCR, suggesting CR/20β-HSD cDNAs are not expressed in this tissue or that the level is below the limits of detectability.

# DISCUSSION

Two closely related CR/20β-HSD cDNAs were cloned from rainbow trout ovarian follicles. Database search shows that they belong to the short-chain dehydrogenase/reductase (SDR) family, with 61% homology to pig 20β-HSD and other mammalian carbonyl reductases at the amino acid level. In the SDR family, two sequences, GlyXXXGlyXGly and TyrXXXLys, which by site-directed mutagenesis (Chen *et al.*, 1990; Chen *et al.*, 1993; Cols *et al.*, 1993) and X-ray crystallographic studies (Varughese *et* al., 1990) have been demonstrated to be in the coenzyme-binding domain and the active site, respectively, are conserved very well. They are strictly conserved in CR/20β-HSD A and B proteins, except that there is a Thr15 in CR/20β-HSD B instead of Ile15 in CR/20β-HSD A and other mammalian CR/20β-HSDs.

In this study, two DNA fragments (termed genes I and II) were also isolated from genomic library, which presumably encode CR/20β-HSD. CR/20β-HSD A cDNA perfectly matched the cDNA sequence deduced from gene I genomic DNA, indicating that gene I encodes CR/20β-HSD A. On the other hand, the sequence differed by two nucleotides between CR/20β-HSD B cDNA and gene II. This discrepancy may reflect gene polymorphism, or alternatively, gene II may encode another CR/20β-HSD different from CR/20β-HSD B. Both genes I and II consist of four exons, with the same exon-intron interruption, but the introns are of different sizes. The human carbonyl reductase gene contains three exons (Forrest *et al.*, 1991), and both human and trout CR/20β-HSD A exhibit similar enzymatic properties, suggesting that the gene duplication and extensive divergence of CR/20β-HSD genes may have occurred early in the vertebrate lineage if they evolved from a common ancestor. There is a TATA box in both 5' flanking regions of CR/20β-HSD gene I and gene II, although they share only 53% sequence identity overall – 700 bp upstream, implying that some other *cis*-elements may regulate the transcription of CR/20β-HSD gene I and II. Interestingly, a candidate site for Ad4BP/SF-1 (Morohashi et al., 1992; Parker et al., 1993), which has been identified as the steroidogenic tissue-specific transcription factor, as well as a potential site for cyclic AMP response element, are found in 5' flanking region of CR/20β-HSD gene I (Fig. 5) by computor search, suggesting that

these regulatory segments specific for sexual differentiation and steroidogenesis may also play a role in the expression of CR/20β-HSDs.

*In vitro* expression in *E. coli* and analysis of the enzymatic properties of the recombinant protein demonstrated that CR/20β-HSD A possesses 20β-HSD as well as other broad CR activity, whereas the CR/20β-HSD B is devoid of activity. It is still unclear whether CR/20β-HSD type B could interfere with the function of CR/20β-HSD type A by competing for its substrates.

The physiological role of CR was thought to be in the NADPH-dependent reduction of a variety of endogenous and foreign carbonyl compounds. However, evidence for its involvement in steroid metabolism is increasing. It has been suggested that two classes of CR exist (Wermuth *et al.*, 1995), one with high activity and steroid specificity and the other with low activity and broad specificity. Pig 20β-HSD and rat ovarian CR seem to belong to the former class. Recombinant rainbow trout CR/20β-HSD A has an enzymatic profile similar to that of pig 20β-HSD, suggesting that it belongs to the steroid specific CR class.

In salmonid fishes, 20β-HSD activity is required for MIH production. Activity in full-grown follicles was elevated by salmon gonadotropin, forskolin and human chorionic gonadotropin *in vitro* (Young *et al.*, 1986). Two CRs have been reported to exist in rat ovary (Aoki *et al.*, 1997), but only one is inducible by pregnant mare's serum gonadotropin (PMSG). The regulation of expression of CR/20β-HSD A by GTH in rainbow trout ovary is now being analyzed (see Chapter III). The involvement and regulation of CR/20β-HSD in the ovary during oocyte maturation could be conserved across the species from fish to mammals.

Rainbow trout CR/20β-HSD A and B differed by only 3 amino acid residues. Two of these residues are located in (I15T) or near (K27Q) GlyXXXGlyXGly, the known cofactor NADPH binding site. These substitutions may cause a conformational change in the binding pocket and interfere with binding of enzyme and co-factor or substrates. Site-directed mutagenesis of these residues is now being conducted to elucidate the critical site for CR/20β-HSD enzyme activity. The results of these experiments will be described in the following chapter (see Chapter II).

Because the cDNAs are so similar, Northern hybridization could not reliably distinguish between CR/20β-HSD A and B mRNAs. Combined with RT-PCR, the results indicate that CR/20β-HSD genes are expressed in a variety of tissues. The significance of such widespread distribution is unclear. However, several studies have reported 20α-HSD and 20β-HSD activity in non-gonadal tissue of several teleosts, including salmonid steroidogenic interrenal tissue (Sangalang and Freeman, 1988; Barry *et al.*, 1997), and salmonid gill, which has been proposed as a site of release of 17α,20β-DP into the environment where it performs a pheromonal function (Kime and Ebrahimi, 1997; Ebrahimi *et al.*, 1996). Thus, our finding of abundant CR/20β-HSD transcripts in gill (and liver) are consistent with these *in vitro* findings. However, rainbow trout tissues such as heart and muscle do not convert 17α-HP to 17α,20β-DP (Ebrahimi *et al.*, 1996), which is consistent with the very low or absent levels of CR/20β-HSD transcript. It is not known whether extra-gonadal tissues are a quantitatively important source of 17α,20β-DP, or if the CR/20β-HSD in extra-gonadal tissues is under the control of reproductive hormones. Conceivably, extra-gonadal CR/20β-HSD could also or alternatively play a more general role in the reduction of a variety of carbonyl compounds. Human and pig CR/20β-HSDs are found in all tissues studied using immunostaining, with high concentration in liver and kidney (Wirth and Wermuth, 1993; Kobayashi *et al.*, 1996).

In conclusion, in this study two closely related cDNAs were isolated from the rainbow trout ovary which encode CR/20β-HSD like proteins. Type A protein exhibits both carbonyl reductase and 20β-HSD activity, while type B protein is devoid of either activity, apparently because of 1-3 amino acid substitutions. Studies in progress are focussed on structure-function relationships of these enzymes, and on their involvement in gonadotropin-induced final oocyte maturation (see Chapters II and III).

# CHAPTER II

## Characterization of the co-enzyme binding site in rainbow trout carbonyl reductase - like 20β-hydroxysteroid dehydrogenases by site-directed mutagenesis

# INTRODUCTION

Rainbow trout ovarian follicle carbonyl reductase - like 20β-hydroxysteroid dehydrogenase (CR/20β-HSD), is an enzyme with the potential physiological role of converting 17α-hydroxyprogesterone (17α-HP) into 17α,20β-dihydroxy-4-pregnen-3-one (17α,20β-DP), the endogenous oocyte maturation-inducing hormone (MIH) of salmonid fishes (Nagahama, 1987), to promote final oocyte maturation (resume the meiosis of oocyte) in salmmonid fish (Nagahama and Adachi, 1985). cDNA cloning indicates that protein products of the two rainbow trout CR/20β-HSD cDNAs obtained share high homology of 61% with mammalian CRs, enzymes which can metabolize steroids, prostaglandins and a variety of carbonyl-containing compounds. Carbonyl reductases belong to the short-chain dehydrogenase/reductases superfamily (SDR) (Jornvall *et al.*, 1995), which contains a large number of prokaryotic and eukaryotic enzymes with different specificities for coenzymes and substrates. Members of the SDR family show amino acid residue identities of 15-30% in general, but share a strictly conserved TyrXXXLys catylytic site, and a Rossmann fold co-enzyme binding domain (Rossmann *et al.*, 1975). In many CRs, the Rossmann fold co-enzyme binding consensus is identified as GlyXXXGlyXGly near the N-terminus. Although CRs purified from several mammalian tissues are monomeric and are NADPH-dependent, enzymes from the lungs of guinea pig, mouse and pig are in tetrameric form (Nakayama *et al.*, 1982; Nakayama and Sawada, 1986; Oritani and Ohya, 1992), with dual coenzyme specificity for NADPH (strongly preferred) and NADH, even though the motif harboring βA and αB has the sequence GlyXXXGlyXGly, whereas GlyXGlyXXGly is usually exhibited by NADH-preferring enzymes. Many studies have demonstrated that Gly in GlyXGlyXXGly fingerprint is the most important residue for NADH-binding. Recombinant proteins with the Gly pattern removed have no enzyme activity (Chen *et al.*, 1990). Restoration of the complete Gly pattern led to an increase of activity (Albalat *et al.*, 1994). Little is known about the critical residues involved and the role of the amino acid GlyXXXGlyXGly fingerprint in determining NADPH-preference. So far, the three dimensional structure of NADPH-preferring SDRs has only been resolved in mouse lung carbonyl reductase by Tanaka *et al.* (1996), in which the determinant for the NADP(H)-preference is the positively charged

environment made by a pair of basic residues (Lys-17 and Arg-39 in MLCR), whereas an Asp at the second β-strand of the βαβ-fold is responsible for the NAD(H)-preference.

In Chapter I, it was shown that trout CR/20β-HSD type B dose not possess either CR or 20β-HSD activity. Among their three distinct amino acids, Ile15 in trout CR/20β-HSD type A is well conserved among many CRs and is located in GlyXXXGlyXGly domain. It is substituted to Thr in CR/20β-HSD type B. To test if this mutation is responsible for abolishing enzyme activities by disturbing the stability of enzyme and co-enzyme complex and further preventing the hybride transferring, a series of studies employing site-directed mutagenesis were conducted and first time confirmed the role of Ile15 in the coenzyme NADPH-binding of trout CR/20β-HSD.

# MATERIALS AND METHODS

***Site-directed mutagenesis***

Point mutations were introduced into the open reading frame (ORF) of CR/20β-HSD type A and type B cDNAs according to the oligonucleotide-directed dual amber method by using a Mutant-Express Km kit (Takara). The mutagenic oligonucleotide was designed to introduce a *Nru*I site without changing the deduced amino acid residues, and to change ATA for Ile to ACA for Thr in CR/20β-HSD type A (termed A/I15T) and ACA for Thr in CR/20β-HSD type B to ATA for Ile (termed B/T15I). The sequences of the mutagenic oligonucleotide are as follows;

5' TCGCGAGTCCTGTGCCTTTATTG 3' for A/I15T,

5' TCGCGAGTCCTATGCCTTTATTG 3' for B/T15I.

ORF fragments containing the introduced *Nru*I site were further subcloned into pET21b+ expression vector using *Nde*I and *Bam*HI as previously described for wild type expression constructs. Dideoxynucleotide sequencing ensured the fidelity of the mutant constructs without any unexpected mutations occurring.

***Expression, purification and characterization of protein samples***

The mutant expression vectors were expressed in *E. coli* (BL21), and overexpressed proteins were purified as previously described for wild type recombinant CR/20β-HSD (Guan *et al.*, 1999). In order to improve the recovery efficiency of mutant proteins, cultures were carried out in a final concentration of 0.1 mM IPTG (1/10 of using for wild type A) at 15°C overnight. The molecular mass of recombinant products from wild types as well as mutants and protein purity were analyzed by SDS polyacrylamide gel electrophoresis on 12.5% gels. Protein concentrations were determined by the method of Bradford (Bio-rad protein assay) using bovine serum albumin as the standard.

***Enzyme kinetic analysis of wild types and mutants***

Enzyme activity was analyzed by using steroid as well as other carbonyl compounds as substrates. For measuring 20β-HSD activity, [$^3$H]-17α-HP (1.48-2.22 TBq/mmol; NEN) was used as substrate. The reaction products were separated using thin-layer chromatography and further confirmed by the recrystallization method described

previously (Guan *et al.*, 1999). For CR activity, enzyme assay was performed using 4-nitrobenzaldehyde as substrate, and enzyme specific activities were measured on a Beckman Du7400 spectrophotometer by observing the rate of change in absorbance of NADPH (0.08 mM) at 340 nm in 1 ml volume at 25°C. Twenty five to 100 µl of enzyme preparation (from 37 to 143 µg/ml) were added to 1 ml assay mixture containing 20 mM Tris-HCl/1 mM EDTA buffer (pH 8.0) with 4-nitrobenzaldehyde (0.5 mM). Reactions were initiated by the addition of 10 µl of NADPH or NADH solution (8 mM), and the absorbance was measured against a blank containing all components except coenzyme. Absorbance of reactions was followed from 1 min to 5 min after addition of NADPH on a Beckman Du 7400 spectrophotometer. Velocities were calculated from the slopes of the zero order portion of the kinetics obtained and were corrected for the control absorbance. One unit of enzyme activity was defined as that amount catalysing oxidation of 1 µmol of NAD(P)H/min at 25°C.

***Determination of binding constants for NADPH by fluorescence titration***

Measurement of the binding constants for NADPH to wild-type CR/20β-HSD type A, type B, mutant A/I15T and mutant B/T15I, were accomplished by titrating the intrinsic protein fluorescence (excitation at 280 nm) on a fluorometer (Shimadzu, FDU-3), following the incremental addition of NADPH (0-2.4 µM) in 20 mM Tris-HCl/1 mM EDTA buffer (pH 8.0) using the method described by Joseph *et al.* (1996). Untransformed fluorescence data were plotted as percent change in fluorescence (%ΔF) at emission $\lambda_{max}$ (316 nm) vs NADPH concentration ([NADPH]). These data were fitted to a saturation absorption isotherm which provided an estimate of the Kd and the associated standard error. These data were transferred using the Lineweaver-Burk equation to generate a linear plot of 1%ΔF vs 1/[NADPH].

# RESULTS

***Construction, site-directed mutagenesis and expression of wild type and mutant CR/20β-HSDs***

The predicted second structure of trout CR/20β-HSD type A and type B proteins are depicted using DNASIS program in Fig 10. Compared with CR/20β-HSD type A and other CRs, the αB of type B is predicted to start from L17 rather than from I15, resulting in the lack of involvement of the second and third Gly of GlyXXXGlyXGly in the αB-helix structure. Since Gly residues in GlyXXXGlyXGly harboring the βAαB turn are known to play an important role in the formation of enzyme-cofactor complex (Tanaka *et al.*, 1995), it is speculated that a less favourable configuration for NADPH binding would be formed in CR/20β-HSD type B.

To test this proposed enzymatic mechanism, I performed site-directed mutagenesis on these two different residues (I15 in type A and T15 in type B) described in the previous analysis of wild type CR/20β-HSD type A and B. An *Nru*I site was co-introduced with a mutated codon in the CR/20β-HSD type A and type B. Mutant clones were isolated by identifying the additional *Nru*I site (shown in Fig. 11), and the authenticity of nucleotide sequence was confirmed (Fig. 12). Mutants and wild type ORFs were subcloned into pET21b+ expression vector to yield pET21b+rcA, pET21b+rcB, pET21b+rcA/I15T and pET21b+rcB/T15I. The wild type and mutant recombinants were overexpressed in BL21 and purified by fast protein liquid chromatography (FPLC) through DEAE Sepharose fast flow (Pharmacia) to yield 50-500 μg for each expressed construct. SDS-PAGE analysis confirmed the purity of each enzyme. Coomassie Brilliant Blue (CBB) staining indicated that the correct protein had been purified even when the mutant enzyme had no detectable activity in a spectrophotometric assay (Fig. 13).

***Enzyme activity for steroid and other carbonyl compounds oxidoreduction***

To assess the effect of each mutation upon steroid reduction, [$^3$H]-labeled 17α-HP was used as a substrate to detect the production of 17α,20β-DP using thin layer chromatography (TLC). Wild type A could convert 17α-HP into 17α,20β-DP, while the mutant A/I15T as well as wild type B failed to produce the 17α,20β-DP, as shown in Fig.

14. However, enzyme activity was recovered in the mutant B/T15I in which Thr15 was replaced by Ile. This observation is consistent with the results from spectrophotometric assay using 4-nitrobenzaldehyde as a substrate, which is a typical substrate for carbonyl reductase (Table 4). Enzyme catalytic efficiency of mutant B/T15I showed silimar to it of wild type A. However, mutant A/I15T reduced the catalytic efficiency by 6.5-fold, wild type B also showed lower efficiency (declined 4.7-fold) comparing to type A.

***The binding of NADPH and formation of enzyme-cofactor-substrate complex***

It was unclear whether the abolition of enzyme activity by substitution of Ile15 to Thr was caused by the inhibition of binding of co-factor or of substrate. To address this question, the binding constants of wild types and mutants for NADPH were measured. The intrinsic fluorescence at 316 (excitation at 280 nm) of the enzyme can be quenched by the addition of NADPH, if the enzyme binds with NADPH as reported by Matsuura *et al.* (1988). Fig. 15 shows the fluorescence emission spectra of wild type CR/20β-HSD type A and B and A/I15T, B/T15I mutants. In contrast to the wild type A, whose λmax decreased corresponding to titration of NADPH, λmax of the wild type B did not change among various concentrations of NADPH. The fluorescence emission spectra of mutant A/I15T was similar to that of wild type B, indicating that the mutant A/I15T could not bind NADPH. However, the fluorescence emission from mutant B/T15I was gradually quenched by titration of NADPH, suggesting that the binding of NADPH occurred. Table 5 summarizes the results of NADPH titration assays of wild type CR/20β-HSDs and mutants A/I15T and B/T15I. The wild-type enzyme CR/20β-HSD type A had a binding constant (Kd) of 0.54 μM, and the B/T15I had a Kd of 0.53 μM. The Kd for wild-type CR/20β-HSD B and mutant A/I15T were 4.87 μM and 6.55 μM, respectively.

# DISCUSSION

Carbonyl reductases belong to the SDR superfamily, which is composed of a large number of prokaryotic and eukaryotic enzymes with different specificties for coenzymes and substrates (Jornvall *et al.*, 1995). Although many CRs have been purified and cDNAs encoding proteins have been cloned, and the primary structures have been determined in mammals, the crystal structure of mouse lung carbonyl reductase (MLCR) determined by X-ray crystallography (Tanaka *et al.*, 1996) is the only three dimensional structure of an NADPH-preferring CR described. Protein-coenzyme interactions are identical among the four subunits in tetrameric MLCR, and four water molecules mediate interactions between NADPH and the enzyme surface. The turn between βA and αB (Gly14-Gly20) harbors the sequence GlyXXXGlyXGly, one of the amino acid fingerprints that comprise the characteristic βαβ dinucleotide-binding motif. It consists of a tight turn at the end of the first strand of a β-sheet and marks the beginnning of the succeeding α-helix, starting from the second glycine. However, based on analysis of trout CR/20β-HSD type B using DNASIS, the substitution of Ile15 to Thr causes the αB helix to start from the residue (Lys17) behind the third glycine (Fig. 10), resulting in changes in spacial conformation of the tight βAαB turn. The second (at the N terminus of the helix) glycine is known to permit the dinucleotide to be bound without obstruction from an amino acid side chain at its position, and the third seems to provide space for a close interaction between the β-strands and the α-helix (Nigel *et al.*, 1990). The conformational change could cause the geometrical re-arrangement of the GlyXXXGlyXGly to a less favourable configuration for NADPH binding. In fact, the kinetic constant (Kd) of mutant A/I15T for NADPH is 10 fold higher than that of the wild type A (Table 2), supporting the idea that substitution of Ile to Thr in trout CR/20β-HSD type B prevents the enzyme from binding NADPH.

In MLCR, eight amino acid residues are involved in enzyme interaction with co-factor through hydrogen bonds forming between NADPH and the enzyme or interaction through four water molecules. Lys17 and Arg39 are two basic residues critical for making electrostatic interactions with the 2'-hposphate group of NADPH. The side chain of Ile19, however, is important for coenzyme binding rather than coenzyme specificity for its direct interaction with the pyrophosphate moiety of NADHP. Any mutation on Ile19 would

destabilize holoenzyme formation (N. Tanaka, personal communication). Ile19 in MLCR is strictly conserved among various mammalian CRs (Fig. 6), with rabbit CR being the only exception, in which it is replaced by valine. Ile19 in MLCR is equivalent to Ile15 in trout CR/20β-HSD type A. It is replaced by threonine in trout CR/20β-HSD type B. Since valine and isoleucine belong to the nonpolar, aliphatic R group of amino acids, while threonine belongs to the polar, uncharged R group. Substitution of valine is considered a milder mutation than that of threonine. In fact, the point mutation of I15/T in type A caused the enzyme to lose its binding affinity by increasing by 10-fold the Kd for NADPH, indicating that Ile15 residue plays an important role in NADPH binding. However, because the cofactor binding site involves contacts with at least eight amino acids in MLCR, it is unlikely that a point mutation of Ile15 can cause gross structural changes in the three-dimensional structure of the enzyme. It is possible that Ile15 interact with other residues to keep the enzyme in a favorable configuration for co-enzyme binding. Further investigation is under way to analyze the consequences of mutation of Ile and other candidate residues on co-enzyme binding.

In the SDR family, enzymes are classified into two groups: one is NADH-preferring, and the other is NADPH-preferring. NAD(H) is a ubiquitous coenzyme involved almost exclusively in biological oxidative degradations that yield ATP, whereas NADP(H) is confined, with few exceptions, to the reactions of reductive biosynthesis. The only distinction between NAD(H) and NADP(H) is the possession of the extra phosphate group by NADP+ that permits biosynthetic enzymes to recognize it. An understanding of how enzymes achieve coenzyme specificity would provide insight into molecular recognition in biochemical reactions. Monomeric CRs purified and cloned from many mammalian tissues are NADPH-dependent SDRs with a conserved motif of GlyXXXGlyXGly fingerprints for co-factor binding. However, some tetrameric CRs show dual co-factor preference. Lys17 and Arg39 in these fingerprints are crucial for NADPH preference. However, this preference could be switched by substitution of Thr38 with Asp in MLCR, suggesting that Asp38 is important for NAD(H) preference (Nakanishi *et al.*, 1996; Nakanishi *et al.*, 1997; Chen *et al.*, 1991). Lys17, Arg39 and Thr38 in MLCR are equivalent to Lys13, Arg35, and Ala34 respectively in trout CR/20β-HSDs. Lys and Arg residues are strictly conserved in trout CR/20β-HSD type A and type B, whereas Thr is replaced by Ala in trout CR/20β-HSDs. The kinetic profile of catalytic analysis also

revealed that trout CR/20β-HSD type A recombinant protein could only catalyze its substrate in the presence of NADPH. It showed no enzyme activity in the reaction with NADH (Table 5), supporting the idea that trout CR/20β-HSD is an NADPH-dependent enzyme.

In conclusion, it was proved in this study that the lack of activity of trout CR/20β-HSD type B is due to the amino acid substitution of Ile15 to Thr. Enzyme activity could be restored by point mutation of T15I in type B. I further showed that Ile15 plays an important role in permitting the enzyme to bind with its co-enzyme, NADPH. The biological significance of this point mutation remains unclear until the biological function and differential expression of trout CR/20β-HSDs are fully elucidated.

# CHAPTER III

## Expression of 3β-hydroxysteroid dehydrogenase, cytochrome P450 aromatase and carbonyl reductase - like 20β-hydroxysteroid dehydrogenases in the ovarian follicle of rainbow trout during oocyte growth and maturation

# INTRODUCTION

Oocyte growth (during which oocytes are arrested in the prophase of the first meiotic division) and meiotic maturation (resumption of the first meiotic division) are two phases during oogenesis in fish. Gonadotropins are thought to control these two processes by regulation of production of two follicular steroidal mediators, estradiol-17β for oocyte growth (Lanzier and MacKay, 1993; Nagahama, 1994) and 17α,20β-DP for oocyte maturation (Nagahama and Adachi, 1985; Young *et al.*, 1983). These steroids are produced from cholesterol via a series of derivatives whose production depends on a cascade of steroidogenic enzymes (Fig. 16). These precursors are converted to estradiol-17β or 17α,20β-DP in granulosa cells. A two-cell type model has been proposed for the production of estradiol-17β and 17α,20β-DP by salmonid ovarian follicles (Young *et al.*, 1986). In this model, GTH acts on the thecal cell layers to promote production of testosterone, the precursor for estradiol-17β, or 17α-HP, the precursor for 17α,20β-DP production through a receptor-mediated adenylate cyclase-cAMP system (Kanamori *et al.*, 1988), while GTH also acts on the granulosa cell layers to enhance 17α,20β-DP production by upregulating 20β-HSD mRNA synthesis (Nagahama *et al.*, 1985) (Fig. 2). Although it is likely that GTH controls steroidogenic enzyme activity through its effects on gene expression, only 20β-HSD activity has been shown to be up-regulated in granulosa cells after GTH stimulation *in vitro*. Neither 3β-HSD nor P450arom activity in granulosa cells has been unequivocally demonstrated to be under GTH control. The granulosa cells are therefore the site of production of the final steroid products controlling vitellogenesis (estradiol-17β) and final oocyte maturation (17α,20β-DP). A number of cDNAs encoding rainbow trout steroidogenic enzymes have been cloned but their expression had only analysed at a few stages of ovarian development (Young *et al.*, 1997). The main aim of the present study was to describe dynamic changes in mRNA levels of 3β-hydroxysteroid dehydrogenase-isomerase (3β-HSD)(Sakai *et al.*, 1994), cytochrome P450 aromatase (P450arom)(Tanaka *et al.*, 1992) and carbonyl reductase-like 20β-hydroxysteroid dehydrogenase (CR/20β-HSD) in ovarian follicles during oocyte growth and oocyte maturation of rainbow trout, with a particular emphasis on changes in mRNA levels of two CR/20β-HSDs whose cDNAs have recently been isolated (Guan *et al.*, 1999; see also

Chapter I in this thesis). *In vitro* studies were also conducted to determine the effect of gonadotropin on steroidogenic enzyme mRNA levels.

# MATERIAL AND METHODS

***Animals collection and samples preparation***

Two-year old rainbow trout were obtained from Samegai Trout Hatchery from May to the end of December in 1996. Samples were classified into four stages based on oocyte size: vitellogenic stages, postvitellogenic stages (migrating germinal vesicle or germinal vesicle breakdown) and postovulatory stages. Samples were frozen in liquid nitrogen and stored at - 80°C before RNA extraction.

The theca and granulosa cell layers of samples at germinal vesicle (GV) and germinal vesicle breakdown (GVBD) stages were separated under a dissecting microscope following established methods (Kagawa *et al.*, 1982). The isolated theca and granulosa layers were washed in Ringer (Kagawa *et al.*, 1982) to remove yolk, a portion was frozen at - 80°C, and the remainder was incubated in plastic tissue culture dishes (6 wells, Costar) containing Ringer, with 1 μg/ml partially purified chum salmon gonadotropin (SGA, Syndel Lab., Vancouver, Canada) for 12 h and 20 h at 15°C in a humidified incubator in an atmosphere of 100% air. 20β-hydroxysteroid dehydrogenase activity was also assessed by incubating tissue in Ringer only, in Ringer plus 100 ng/ml 17α-HP (Sigma), in Ringer with GTH, and in Ringer with 17α-HP plus GTH. Triplicate incubations were made for each treatment. The incubation media were frozen until radioimmunoassay for 17α,20β-DP was conducted.

***Extraction of poly(A)$^+$ RNA and Northern blot hybridization***

Total RNAs from intact ovarian follicles at various stages were prepared using ISOGEN (Nippon Gene), and poly(A)$^+$ RNAs were purified using Oligotex-DT30 (Takara). The poly(A)$^+$ RNAs (2 μg) were electrophoresed on a 1.5% (w/v) formaldehyde denaturing gel and blotted onto a nylon membrane (Hybond N$^+$, Amersham). The membrane was rinsed briefly and subsequently baked at 80°C for 30 min.

The probes used for hybridization were prepared as follows: The full length (1.37 kb) of 3β-HSD cDNA fragment was cut out at the *Eco*RI cloning site and purified with a GENECLEAN II Kit (BIO 101), and then labeled with [α-$^{32}$P]-dCTP using a Random Labeling Kit (Promega). Probes for P450arom and 20β-HSD mRNAs were labelled with

[$\alpha$-$^{32}$P]-dCTP using PCR amplification of the 5'-end of P450arom cDNA (1-572), and 20$\beta$-HSD type A (1-532), respectively. The authenticity of probes was confirmed by their recognition of template cDNA clones.

Hybridizations were carried out under high stringency conditions of 5 x SSC, 35% formamide, 5 x Denhardt's, 10% Dextran sulfate, 0.1% (w/v) SDS, and 100 mg/ml herring sperm DNA, with 1 x $10^6$ c.p.m. of the probe incubated at 45°C overnight. After washing with 1 x SSC, 0.1% (w/v) SDS at 60°C twice for 20 min each, the membrane was exposed to an imaging plate for one day and analyzed by a BAS 2000 image analyzer (FUJI Photo Film Co. Ltd., Tokyo, Japan).

***Reverse-transcription and polymerase chain reaction (RT-PCR)***

Two cDNAs (type A and type B) encoding CR/20$\beta$-HSD proteins have recently been isolated from rainbow trout ovary (see Chapter I). Their mRNAs can not be reliably distinguished because of their very high homology. To determine which CR/20$\beta$-HSD is stimulated by GTH, RT PCR was performed using primer sets which specifically recognized template type A or type B. One microgram of total RNA extracted from granulosa cells and theca cells was reverse-transcribed to first-strand cDNA using a cDNA Synthesis Kit (Takara). A portion (1/25) of the reaction mixture was subjected to PCR amplification. The specific primer set for type A was:
5'-TCACCAGCACAGCTAATTACATTATTTAAACCAGAGTTG (35-73)-3' and
5'-CATTCACCACTCTGGCATTTGG (511-532).
The specific primer set for type B was: 5'-CTACAACCACAGTGCGGT (22-39) and 5'-CATTCACCACTCTGGCATTTGG (502-523). PCR reaction was performed at 94°C for 1 min, 62°C for 1 min and 72°C for 1 min for 25 cycles using a Perkin-Elmer 480 thermal cycler.

***Antibody production***

C-terminus peptide of CR/20$\beta$-HSD type A (CEGAKEPHGQLVWDKTVQE) was synthesized by the F-moc protocol on an Applied Biosystem model 431A peptide synthesizer, and purified by reversed-phase HPLC using a ODS-5 column (Develosil). To increase antigenicity, the peptide was coupled to bovine serum albumin (BSA: Fraction V,

Sigma), using EMCS (N-(e-Maleimidocaproyloxy)succinimide) (Dojindo), following the cleavage of disulfide bonds within the molecule of BSA with dithiothreitol (DTT).

Three mice were immunized at 2-week intervals by subcutaneous injections of peptide-linked protein (100 μg/mouse/injection). The antigen was emulsified in Freund's complete adjuvant at the first injection and Freund's incomplete adjuvant after the first injection. The whole blood from mice were collected one week after the last injection, and serum was separated by centrifugation and kept at - 80°C. An antibody against 3β-HSD (anti-tr3β-HSD-M) was raised in rabbits by Kobayashi *et al.* (1998).

***Western blot***

SDS/polyacrylamide gel electrophoresis was carried out on 12.5 % acrylamide gels in the presence of 0.1% SDS. Proteins were blotted on PVDF (Millipore) using an electroblotting apparatus (NIPPON EIDO). The membrane was rinsed in Tris-buffered saline (TBS: 20 mM Tris-HCl, 150 mM NaCl, pH 7.5), blocked with non-fat dry milk in TBS containing 0.1% Tween 20 (TTBS). After washing three times (5 min each) with TTBS, the membrane was incubated with a 1:1000 dilution of anti-CR/20β-HSD C-terminus antibody or anti-tr3β-HSD-M at 4°C overnight, and washed with TTBS three times, then incubated against the second antibody (goat anti-mouse or goat anti-rabbit conjugated with alkaline phosphatase) (ZYMEL, USA). Following three washes with TTBS, phosphatase activity was visualized by treating the membrane with 0.2 mM 5-bromo-4-chloro-3-indolylphosphate p-toluidine salt and nitroblue tetrazolium (Sigma) in 100 mM diethanolamine buffer (pH 9.5) containing 5 mM $MgCl_2$.

# RESULTS

## *Dynamic changes of mRNAs for 3β-HSD, P450arom, CR/20β-HSD and GTH II receptors in rainbow trout ovary during oocyte growth and oocyte maturation*

RNAs were extracted from different stages of rainbow trout ovarian follicles. Northern analysis was performed to determine the expression of steroidogenic enzymes during oocyte growth and maturation. Fig. 17 shows that the 3β-HSD gene was expressed at low levels during the vitellogenic stages, but mRNA levels increased and reached a peak at the time of oocyte maturation. Transcripts of 3β-HSD remained highly after ovulation. P450arom mRNA levels were high in ovarian follicles during active vitellogenesis which was maintained until the postvitellogenic stage. When oocytes entered the oocyte maturation stage, the expression of P450arom dramatically decreased with undetectable levels in postovulatory follicles. The expression of CR/20β-HSD genes (the probe used cannot distinguish between CR/20β-HSD type A and type B) was low in ovarian follicles during active vitellogenesis. Expression markedly increased in postvitellogenic follciles during oocyte maturation which was maintained in postovulatory follicles. Northern blot analysis of GTH II receptor gene using rainbow trout cDNA probes, which were kindly provided by Dr. Y. Oba in our laboratory, showed that expression pattern of GTH II receptor mRNAs paralleled that of P450arom gene and reached a peak in the late vitellogenic stage. However, unlike P450arom, gene expression was maintained in maturing and postovulatory stages. The quantity of each enzyme mRNA normalized to rainbow trout β-actin transcripts is shown in Fig. 18.

## *Changes in expression of steroidogenic enzyme genes in granulosa cells*

Postvitellogenic ovarian follicular tissue with immature but fully-grown follicles were physically separated into two layers, granulosa layers and theca layers. The radioimmunoassay data (Fig. 19) indicated that 20β-HSD activity in granulosa cells was highly stimulated by GTH *in vitro*, as assessed by conversion of 17α-HP to 17α,20β-DP. 17α,20β-DP production from incubation of granulosa cells with SGA(GTH) and 17α-HP was 12-fold higher than that from incubation of granulosa cells with only 17α-HP.

Northern blot analysis of mRNA from these isolated granulosa cells showed that GTH stimulated a 3.5 fold increase in CR/20β-HSD transcripts, but decreased 3β-HSD expression in granulosa cells (Fig. 20). To address which CR/20β-HSD gene (type A or type B) was stimulated by GTH treatment, RT-PCR was carried out and the result is shown in Fig. 21. CR/20β-HSD type A mRNA levels increased after GTH stimulation, while CR/20β-HSD type B mRNA levels did not change in response to GTH *in vitro*. Therefore, the increase in CR/20β-HSD transcripts in response to GTH found by Northern blot analysis can be attributed to a specific effect of GTH on CR/20β-HSD type A gene expression.

***Western blot analysis of 3β-HSD and 20β-HSD in granulosa cells***

To demonstrate that CR/20β-HSD protein(s) increase after GTH stimulation, an antibody against CR/20β-HSD C-terminus was raised and Western blotting was conducted (Fig. 22). The intensity of the 45 kDa band representing 3β-HSD did not change between samples incubated with or without GTH, but the immunoreactive 30 kDa band of CR/20β-HSD was darkly stained after GTH stimulation, indicating that CR/20β-HSD protein production increased in response to GTH.

# DISCUSSION

Oocyte maturation is a prerequisite process for the successful fertilization. Pituitary LH and progestogens are believed to play important roles in inducing oocyte maturation in vertebrates including mammals. However, the chemical identification of maturation-inducing hormone (steroid) has so far been limited only to fish oocytes, although progesterone has long been considered to be a MIH in frog oocytes (Nagahama and Adachi, 1985; Nagahama, 1987). For this reason, the mechanisms of MIH production have been studied mainly using fish ovarian follicles. The present study provides, for the first time, molecular data depicting the dynamic changes of expression of various steroidogenic enzyme genes involved in oocyte maturation. These data allow the further development of models previously presented for the production of ovarian steroids in salmonids (Nagahama, 1994).

A model for maturation-inducing hormone production in the salmonid follicle was proposed by Young *et al.* (1986). During vitellogenesis, the outer thecal layer of the ovarian follicles produces testosterone which is then converted to estradiol-17β by P450arom in the inner granulosa layer. However, in late vitellogenic stage, P450arom activity in granulosa cells decreases rapidly. The declining estradiol-17β levels, a consequence of reduced granulosa cell P450arom activity, results in GTH increases in the plasma of salmonids via release of the hypothalamo-hypophysial system from negative feedback. The GTH surge occurs just prior to the initiation of GVBD (Fostier *et al.*, 1983; Young *et al.*, 1983). Gonadotropin acts directly on both granulosa cells and theca cells. On the one hand, GTH stimulates the synthesis and secretion of two major products, testosterone and 17α-HP, from the steroidogenic special thecal cells (Nagahama, 1984). On the other hand, GTH acts on the granulosa cells to stimulate the conversion of 17α-HP to 17α,20β-DP by enhancing 20β-HSD activity through a mechanism involving cAMP-dependent RNA synthesis (Kanamori and Nagahama, 1988; Nagahama *et al.*, 1985). The decrease of 17α-hydroxylase/C17-20-lyase and P450arom activity prior to the maturation stage results in decreased estradiol-17β production, and the increase in 20β-HSD activity enhances the conversion of 17α-HP to 17α,20β-DP, the MIH which binds to an oocyte

membrane bound receptor and then reinitiates the meiosis of prophase-arrested oocytes (Nagahama *et al.*, 1995; Nagahama, 1997).

In the present study, 3β-HSD mRNA levels were barely detected during vitellogenesis, but increased and reached a peak in oocyte maturation, and remained high levels after ovulation. Since 3β-HSD activity is required in the synthesis of progesterone, 17α-HP and testosterone, the increase in 3β-HSD mRNA levels results in a greater capacity of 17α-HP and testosterone, the precursors of 17α,20β-DP and estradiol-17β, respectively. These Northern blot results correspond with results from Sakai *et al.* (1994), except they found 3β-HSD markedly decreased in postovulatory tissue, whereas I did not find much decrease in mRNA levels. Since the steroidogenic capacity of the salmonid ovarian follicle declines within a few days after ovulation, differences in the age of postovulatory follicles in these two studies may account for this divergence in results.

Northern blot analysis also showed that P450arom mRNA levels were high during vitellogenesis and declined dramatically prior to GVBD, when the expression of GTH II receptor gene in granulosa cells increases. This is consistent with several previous studies which have demonstrated that P450arom activity (the capacity to produce estradiol-17β in response to exogenous testosterone) in granulosa cells increases during vitellogenesis and decreases rapidly in association with the ability of the oocytes to mature in response to GTH (Kagawa *et al.*, 1983; Young *et al.*, 1983; Nagahama, 1994). Further studies are required to determine factors responsible for the regulation of the rapid decrease in P450arom gene expression in granulosa cells immediately prior to oocyte maturation.

In contrast to the change in P450arom gene expression, CR/20β-HSD mRNA levels markedly increased in both postvitellogenic follicles undergoing GVBD and postovulatory follicles. These Northern hybridization data are in good agreement with previous incubation studies showing that immediately prior to oocyte maturation, intact ovarian follicles acquire an increased ability to produce 17α,20β-DP in response to 17α-HP (Young *et al.*, 1983). Earlier incubation studies using thecal and granulosa cell layers have shown tht the site of 20β-HSD is restricted mainly to granulosa cells and thus 17a,20β-DP synthesis occurs in granulosa cells (Young *et al.*, 1986). The results of this study also confirm the site of CR/20β-HSD in granulosa cells, although no attempt was made to determine whether CR/20β-HSD is also present in thecal cells. A major finding in this

study is that GTH enhances CR/20β-HSD gene expression in granulosa cells isolated from postvitellogenic follicles. Western blot results also showed that CR/20βHSD protein contents were elevated by GTH treatment. The substantial increase in expression of CR/20β-HSD gene in granulosa cells by GTH treatment provides the molecular basis for the ability of ovarian follicles to rapidly produce large quantities of 17α,20β-DP over a relatively short time-frame during GTH-induced oocyte maturation.

It should be emphasized that CR/20β-HSD type A gene, but not type B gene, is inducible by GTH stimulation. Since CR/20β-HSD type A exhibits 20β-HSD activity, the enhanced expression of CR/20β-HSD type A gene increases the conversion of 17α-HP to MIH. The existence of two CRs has also been reported in rat ovary. One is inducible by pregnant mare's serum gonadotropin while the other is not (Aoki *et al.*, 1997). Several reports indicate that CR in rat ovary is involved in ovulatory processes (Iwata *et al.*, 1989; Inazu *et al.*, 1992; Toft *et al.*, 1994), and a recent report found that CR plays a role in prostaglandin metabolism in theca cells (Okita *et al.*, 1996; Iwata *et al.*, 1990).

The GTH-induced CR/20β-HSD gene and protein expression in granulosa cells is consistent with earlier *in vitro* experiments showing that both actinomycin D and cycloheximide reduced the enhancing effect of GTH on 20β-HSD (Nagahama *et al.*, 1985). The GTH effect on CR/20β-HSD could be mimicked by dibutyryl cyclic AMP, by phosphodiesterase inhibitors, and by forskolin, an activator of adenylate cyclase, suggesting that the enhancing effect of GTH involves a cyclic AMP-dependent step (Kanamori and Nagahama, 1988). The 5' upstream flanking region of CR/20β-HSD type A gene contains a potential cyclic AMP response element (CRE) at about 300 bp beyond the TATA box. A possible Ad4BP/SF-1 site is also present. However, it is of interest to note that neither CRE nor Ad4BP/SF-1 site occurs in the upstream region of CR/20β-HSD type B gene. The distinct effect of GTH on CR/20β-HSD type A and type B gene expression is therefore thought to be due to their different promoter segments. The details of regulation of the respective genes as well as the functional significance of CR/20β-HSD type B are currently being studied.

In summary, in this study, changes in 3β-HSD, P450arom, and 20β-HSD steroidogenic enzyme genes expression and GTH II receptor gene expression were correlated with oocyte growth and oocyte maturation. In the vitellogenic stage, 3β-HSD and P450arom mRNA levels increase gradually, and P450arom mRNA peaks just before the oocyte enters the maturation phase, while estradiol-17β production by the follicle is maximum. At that time, GTH II receptor gene is expressed in the granulosa cells, and presumably leads to increased sensitivity of granulosa cells to GTH stimulation. When P450arom mRNA and protein decline and GTH II receptor mRNA reaches its peak in granulosa cells, GTH acts on the granulosa cells to increase CR/20β-HSD type A gene expression, and enhances the 20β-HSD activity in granulosa cells. These dynamic changes in gene expressions therefore prove the basis for the shift in steroidogenesis from estradiol-17β production to 17α,20β-DP production occurring immediately prior to oocyte maturation, thus reinitiating oocyte meiosis and leading to final oocyte maturation and subsequent ovulation. Elucidation of mechanisms regulating P450arom and 20β-HSD gene expression, particularly the effects of GTH on the promoter regions of these genes, will provide further understanding of steroid and protein hormone modulation of steroidogenic enzymes. These studies will certainly provide the basis for a study at the molecular levels of hormonal regulation of germ cell (oocyte) development and maturation.

## ACKNOWLEDGMENTS

I wish first to thank Professor Yoshitaka Nagahama throughout my graduate studies. I also thank my graduate committee: Professor Naoto Ueno, Professor Tetsuo Yamamori and Professor Kenichiro Morohashi for their advice. I feel very grateful to Dr. M. Yoshikuni, Dr. M. Tanaka, Dr. G. Young, Dr. T. Kobayashi, Dr. T. Todo, Dr. Y. Katsu, Dr. D. Kobayashi, and Dr. Y. Oba for their kind advice and continuous encouragement. Many thanks are also extended to all the members of the laboratory of reproductive Biology, National Institute for Basic Biology.

# REFERENCES


Albalat, R., Atrican, S., and Gonzalez-Duarte, R. (1994). *Drosophila lebanonensis* ADH: analysis of recombinant wild-type enzyme and site-directed mutants/The effect of restoring the consensus sequence in two positions. *FEBS Lett. 341*, 171-176.

Aoki, H., Okada, T., Mizutani, T., Numata, Y., Minegishi, T., and Miyamoto, K. (1997). Identification of two closely related genes, inducible and noninducible carbonyl reductases in the rat ovary. *Biochem. Biophys. Res. Comm. 230*, 518 - 523.

Axelrod, L.R., Mattijssen, C., Goldzieher, J.W., and Pulliam, J.E. (1965). Definitive identification of microquantities of radioactive steroids by recrystallization to constant specific activity. *Acta Endocrinol. 99*, 7-77.

Barry, T.P., Riebe, J.D., Parrish, J.J., and Malison, J.S. (1997). Effects if 17α,20β-dihydroxy-4-pregnen-3-one on cortisol production by rainbow trout interrenal tissue *in vitro*. *Gen. Comp. Endocrinol. 107*, 172-181.

Chen, Z., Lee, W. R., and Chang, S. H. (1991). Role of aspartic acid 38 in the cofactor specificity of *Drosophila* alcohol dehydrogenase. *Eur. J. Biochem. 202*, 263-267.

Chen, Z., Lu, L., Shirley, M., Lee, W.R., and Chang, S.H. (1990). Site-directed mutagenesis of glycine-14 and two "critical" cysteinyl residues in *Drosophila* alcohol dehydrogenase. *Biochemistry 29*, 1112-1118.

Chen, Z., Jiang, J. C., Lin, Z. G., Lee, W. R., Baker, M. E., and Chang, S. H. (1993). Site-specific mutagenesis of *Drosophila* alcohol dehydrogenase: evidence for involvement of tyrosine-152 and lysine-156 in catalysis. *Biochemistry 32*, 3342-3346.

Cols, N., Marfany, G., Atrian, S., and Gonzalez-Duarte, R. (1993). Effect of site-directed mutagenesis on conserved positions of *Drosophila* alcohol dehydrogenase. *FEBS Lett. 319*, 90-94.

Ebrahimi, M., Scott, A.P., and Kime, D.E. (1996). Extragonadal production of 17α,20β-dihydroxy-4-pregnen-3-one *in vitro* in cyprinid fish. *Gen. Comp. Endocrinol. 104*, 296-303.

Fostier, A., Jalabert, B., Billard, R., Breton, B., and Zohar, Y. (1983). The gonadal steroidogenesis. *In "Fish Physiology"* (W. S. Hoar, D. J. Randall, and E. M. Donaldson, eds.), Vol. IX A, pp. 277-372. Academic Press, New York.

Guan, G. J., Tanaka, N., Todo, T., Young, G., Yoshikuni, M., and Nagahama, Y. (1999). Cloning and expression of two carbonyl reductase-like 20β-hydroxysteroid dehydrogenase cDNAs in ovarian follicles of rainbow trout (*Oncorhynchus rhodurus*). Biochem. Biophys. Res. Comm. (in press).

Inazu, N., Inaba, N., Satoh, T., and Fujii, T. (1992). Human chorionic gonadotropin causes an estrogen-mediated induction of rat ovarian carbonyl reductase. *Life Sci. 51*, 817-822.

Iwata, N., Inazu, N., and Satoh, T. (1989). The purification and properties of NADPH-dependent carbonyl reductases from rat ovary. *J. Biochem.* (Tokyo) *105*, 556-564.

Iwata, N., Inazu, N., and Satoh, T. (1990). Changes and localization of ovarian carbonyl reductase during pseudopregnancy and pregnancy in rats. *Biol. Reprod. 43*, 397-403.

Jez, J.M., Schlegel, B.P., and Penning, T.M. (1996). Characterization of the substrate binding site in rat liver 3α-hydroxysteroid/dihydrodiol dehydrogenase. *J. Biol. Chem. 271*, 30190-30198.

Jornvall, H., Persson, B., Krook, M., Atrian, S., Gonzalez-Duarte, R., Jeffery, J., and Ghosh, D. (1995). Short-chain dehydrogenase/reductases (SDR). *Biochemistry 34,* 6003 - 6013.

Kagawa, H., Young, G., and Nagahama, Y. (1983). Relationship between seasonal plasma estradiol-17β and testosterone levels and *in vitro* production by ovarian follicles of amago salmon (*Oncorhynchus rhodurus*). *Biol. Reprod. 29*, 301-309.

Kagawa, H., Young, G., Adachi, S., and Nagahama, Y. (1982). Estradiol-17β production in amago salmon (*Oncorhynchus rhodurus*) ovarian follicles: Role of the thecal and granulosa cells. *Gen. Comp. Endocrinol. 47*, 440-448.

Kanamori, A., & Nagahama, Y. (1988). Involvement of 3',5'-cyclic adenosine monophosphate in the control of follicular steroidogenesis of amago salmon (*Oncorhynchus rhodurus*). *Gen. Comp. Endocrinol. 72*, 39 - 53.

Kawauchi, H., Suzuki, K., Itoh, H., Swanson, P., Naito, N., Nagahama, Y., Nozaki, M., Nakai, Y., and Itoh, H. (1989). The duality of teleost gonadotropins. *Fish Physiol. Biochem. 7*, 29-38.

Kime, D.L., and Ebrahimi, M. (1997). Synthesis of 17,20α- and 17,20β-dihydroxy-4-pregnen-3-one, 11-ketotestorsterone and their conjugates by gills of teleost fish. *Fish Physiol. Biochem. 17*, 117-121.

Kobayashi, K., Ohno, S., Shinoda, M., Toyoshima, S., and Nakajin, S. (1996). Immunochemical distribution and immunohistochemical localization of 20beta-hydroxysteroid dehydrogenase in neonatal pig tissues. *J. Steroid Biochem. Mol. Biol. 59*, 485-493.

Kobayashi, T., Nakamura, M., Kajiura-Kobayashi, H., Young, G., and Nagahama, Y. (1998). Immunolocalization of steroidogenic enzymes (P450scc, P450c17, P450arom, and 3βeta-HSD) in immature and mature testes of rainbow trout (*Oncorhynchus mykiss*). *Cell Tissue Res. 292*, 573-577.

Lanzier, C. B., and MacKay, M. E. (1993). Vitellogenin gene expression in teleost fish. *In "Biochemistry and Molecular Biology of Fishes"* (P.W. Hochachka and T.P. Mommsen, eds.), Vol. 2, Elsevier Biomedical Publishers, New York.

Masui, Y., and Clarke, H.J. (1979). Oocyte maturation. *Int. Rev. Cytol. 57*, 185-282.

Matsuura, K., Nakayama, T., Nakagawa, M., Hara, A., and Sawada, H. (1988). Kinetic mechanism of pulmonary carbonyl reductase. *Biochem. J. 252*, 17-22.

Morohashi, K., Honda, H., Inamata, Y., Handa, H., and Omura, T. (1992). A common trans-acting factor, Ad4-binding protein, to the promoters of steroidogenic P-450s. *J. Biol. Chem. 267*, 17913-17919.

Nagahama, Y. (1984). Mechanism of gonadotropin control of steroidogenesis in the teleost ovarian follicle. *Gunma Symp. Endocrinol. 21*, 167-182.

Nagahama, Y. (1987). Endocrine control of oocyte maturation. *In "Hormones and Reproduction in Fishes, Amphibians, and Reptiles"* (D.O. Norris, and R.E. Jones, eds.), pp. 171-202. Plenum Press, New York.

Nagahama, Y. (1994). Endocrine regulation of gametogenesis in fish. *Int. J. Dev. Biol. 38*, 217-229.

Nagahama, Y. (1997). 17a,20b-Dihydroxy-4-pregnen-3-one, a maturation-inducing hormone in fish oocytes: Mechanisms of synthesis and action. *Steroids 62*, 190-196.

Nagahama, Y., and Adachi, S. (1985) Identification of maturation-inducing steroid in a teleost, the amago salmon (*Oncorhynchus rhodurus*). *Dev. Biol. 109,* 425 - 435.

Nagahama, Y., Kagawa, H., and Young, G. (1985). Stimulation of 17α,20β-dihydroxy-4-pregnen-3-one production in the granulosa cells of amago salmon, *Oncorhynchus rhodurus*, by cyclic nucleotides. *J. Exp. Zool. 236*, 371-375.

Nagahama, Y., Kagawa, H., and Young, G. (1985). Effect of actinomycin D and cycloheximide on gonadotropin-induced 17α,20β-dihydroxy-4-pregnen-3-one production by intact follicles and granulosa cells of the amago salmon, *Oncorhynchus rhodurus*. *Dev. Growth Differ. 27*, 213-221.

Nagahama, Y., Yoshikuni, M., Yamashita, M., Tokumoto, T., and Katsu, Y. (1995). Regulation of oocyte growth and maturation in fish. *Curr. Top. Dev. Biol. 30*, 103-145.

Nakajin, S., Tamura, F., Takase, N., and Toyoshima, S. (1997). Carbonyl reductase activity exhibited by pig testicular 20 beta-hydroxysteroid dehydrogenase. *Biol. Pharm. Bull. 20*, 1215-1218.

Nakanishi, M., Matsuura, K., Kaibe, H., Tanaka, N. (1997). Switch of coenzyme specificity of mouse lung carbonyl reductase by substitution of threonine 38 with aspartic acid. *J. Biol. Chem. 202*, 2218-2222.

Nakanishi, M., Kaibe, H., Matsuura, K., Kakumoto, M., Tanaka, N., Nonaka, T., Mitsui, Y., and Hara, A. (1996). Site-directed mutagenesis of residues in coenzyme-binding domain and active site of mouse lung carbonyl reductase. *Enzymol. Mol. Biol. Carbonyl Metab. 6*, 555-561.

Nakayama, T., Hara, A., and Sawada, H. (1982). Purification and characterization of a novel pyrazole-sensitive carbonyl reductase in guinea pig lung. *Arch. Biochem. Biophys. 217*, 564-573.

Nakayama, T., and Sawada, H. (1986). Characterization of pulmonary carbonyl reductase of mouse and guinea pig. *Biochem. Biophys. Acta 882*, 220-227.

Nigel, S. S., Alan, B., and Richard, N. P. (1990). Redesign of the coenzyme specificity of a dehydrogenase by protein engineering. *Nature 343*, 38-43.

Okita, R. T., and Okita, J. R. (1996). Prostaglandin-metabolizing enzymes during pregnancy: characterization of NAD(+)-dependent prostaglandin dehydrogenase, carbonyl reductase, and cytochrome P450-dependent prostaglandin omega-hydroxylase. *Crit. Rev. Biochem. Mol. Biol. 31*, 101-126.

Oritani, H., and Ohya, I. (1992) Purification and characterization of pig lung carbonyl reductase. *Arch. Biochem. Biophys. 292*, 539-547.

Parker, K. L., and Schimmer, B. P. (1993) Transcriptional regulation of the adrenal steroidogenic enzymes. *Trends Endocrinol. Metab. 4*, 46-50.

Rossmann, M. G., Liljas, A., Branden, C. I., and Banaszak, L. J. (1975). Evolutionary and structural relationships among dehydrogenases. *In "The Enzymes"* (P.D. Boyer, ed.), pp. 61-102, Academic Press, New York.

Sakai, N., Tanaka, M., Takahashi, M., Fukada, S., Mason, J.I., and Nagahama, Y. (1994). Ovarian 3β-hydroxysteroid dehydrogenase/$\Delta^5$-$\Delta^4$ isomerase of rainbow trout: its cDNA cloning and properties of the enzyme expressed in a mammalian cell. *FEBS Lett. 350*, 309-313.

Sangalang, G.B., and Freeman, H.C. (1988). *In vitro* biosynthesis of 17α,20β-dihydroxy-4-pregnen-3-one by the ovaries, testes and head kidneys of the Altantic salmon *Salmo salar. Gen. Comp. Endocrinol. 69*, 406-415.

Swanson, P. (1991). Salmon gonadotropins: reconciling old and new ideas. *In "Proc. the IVth International Symposium on Reproductive Physiology of Fish"* (A.P. Scott, J.P., Sumpter, D.E., Kime, and M.S. Rolfe, eds.), pp. 2-7. Fish Symp. 91, Sheffield.

Tanaka, M., Nakajin,S., Kobayashi, D., Fukada, S., and Nagahama, Y. (1996). Carbonyl reductase is a major enzyme involved in production of maturation inducing hormone in ayu (*Plecoglossus altivelis*) ovarian follicles. Abstract, 3rd International Symposium on Fish Endocrinology, p. 73.

Tanaka, M., Ohno, S., Adachi, S., Nakajin, S., Shinoda, M., and Nagahama, Y. (1992). 20β-hydroxysteroid dehydrogenase of neonatal pig testis: purification and some properties. *J. Biol. Chem. 267*, 13451 - 13455.

Tanaka, M., Telecky, T. M., Fukada, S., Adachi, S., Chen, S., and Nagahama, Y. (1992). Cloning and sequence analysis of the cDNA encoding P-450 aromatase (P450arom) from a rainbow trout (*Oncorhynchus mykiss*) ovary; relationship between the amount of P450arom mRNA and the production of oestradiol-17β in the ovary. *J. Mol. Endocrinol.*, 8, 53-61.

Tanaka, N., Nonaka, T., Nakanishi, M., Deyashiki, Y., Hara, A., and Mitsui, Y. (1995). Crystallization of mouse lung carbonyl reductase complexed with NADPH and analysis of symmetry of its tetrameric molecule. *J. Biochem. 118*, 871-873.

Tanaka, N., Nonaka, T., Nakanishi, M., Deyashiki, Y., Hara, A., and Mitsui, Y. (1996). Crystal structure of the ternary complex of mouse lung carbonyl reductase at 1.8 A resolution: the structural origin of coenzyme specificity in the short-chain dehydrogenase/reductase family. *Structure 4*, 33-45.

Toft, E., Soderstrom, M., Ahlberg, M.B., and DePierre, J.W. (1994). A novel 34 kDa glutathione-binding protein in mature rat ovary. *Biochem. Biophys. Res. Comm.* 201, 149-154.

Varughese, K.I., Xuong, N.H., Kiefer, P.M., Matthews, D.A., and Whiteley, J.M. (1994). Structural and mechanistic characterization of dihydropteridine reductase: A member of the Tyr-$(Xaa)_3$-Lys-containing family of reductases and dehydrogenases. *Proc. Natl. Acad. Sci. USA, 91*, 5582-5586.

Wasserman, W.J., and Smith, L.D. (1978). Oocyte maturation in nonmammalian vertebrates. *In "The Vertebrate Ovary"* (R.E. Jones, ed.), pp. 443-468. Plenum Press, New York.

Wermuth, B., Bohren, K. M., Heinemann, G., von Wartburg, J-P., and Gabbay, K. H. (1988). Human carbonyl reductase: nucleotide sequence analysis of a cDNA and amino acid sequence of the encoded protein. *J. Biol. Chem. 263*, 16185 - 16188.

Wermuth, B., Mader-Heineman, G., and Ernst, E. (1995). Cloning and expression of carbonyl reductase from rat testis. *Eur. J. Biochem. 228*, 473 - 479.

Wirth, H., and Wermuth, B. (1992) Immunohistological localization of carbonyl reductase in human testis. *J. Histochem. Cytochem. 40*, 1857 - 1863.

Yamashita, M., Kajiura, H., Tanaka, T., Onoe, S., and Nagahama, Y. (1995). Molecular mechanisms of the activation of maturation-promoting factor during goldfish oocyte maturation. *Dev. Biol. 168*, 62-75.

Young, G., Kagawa, H., and Nagahama, Y. (1983). Evidence for a decrease in aromatase activity in the ovarian granulosa cells of amago salmon (*Oncorhynchus rhodurus*) associated with final oocyte maturation. *Biol. Reprod. 29*, 310-315.

Young, G., Adachi, S., and Nagahama, Y. (1986). Role of ovarian thecal and granulosa layers in gonadotropin-induced synthesis of a salmonid maturation-inducing substance (17α,20β-dihydroxy-4-pregnen-3-one). *Dev. Biol. 118*, 1 – 8.

Young, G., Crim, L. W., Kagawa, H., Kambegawa, A., and Nagahama, Y. (1983). Plasma 17α,20β-dihydroxy-4-pregnen-3-one levels during sexual maturation of amago salmon (*Oncorhynchus rhodurus*): Correlation with plasma gonadotropin and *in vitro* production by ovarian follicles. *Gen. Comp. Endocrinol. 51*, 96-105.

Young, G., Todo, T., Kobayashi, T., Guan, G., and Nagahama, Y. (1997). Steroidogenesis by the salmonid ovarian follilce: the two-cell type model revisited. *In "Advances in Comparative Endocrinology"* (S. Kawashima, and S. Kikuyama, (ed.),. pp. 1443-1449. Monduzzi Editore, Bologna, Italy.

# FIGURES AND TABLES

Fig. 1 Endocrine control of oocyte growth and maturation in fish. Oogenesis in teleost fish is composed of two phases, vitellogenesis and oocyte maturation. Estradiol-17β produced from ovarian follicles promotes hepatic synthesis and secretion of vitellogenin via the vascular system. 17α,20β-dihydroxy-4-pregnen-3-one (17α,20β-DP, an identified maturation-inducing hormone in fish oocytes) is rapidly synthesized to reinitiate the meiosis of oocyte (oocyte maturation). Gonadotropin is responsible for production of estradiol-17β and 17α,20β-DP and for switching from vitellogenesis to oocyte maturation by activation of 20β-hydroxysteroid dehydrogenase.

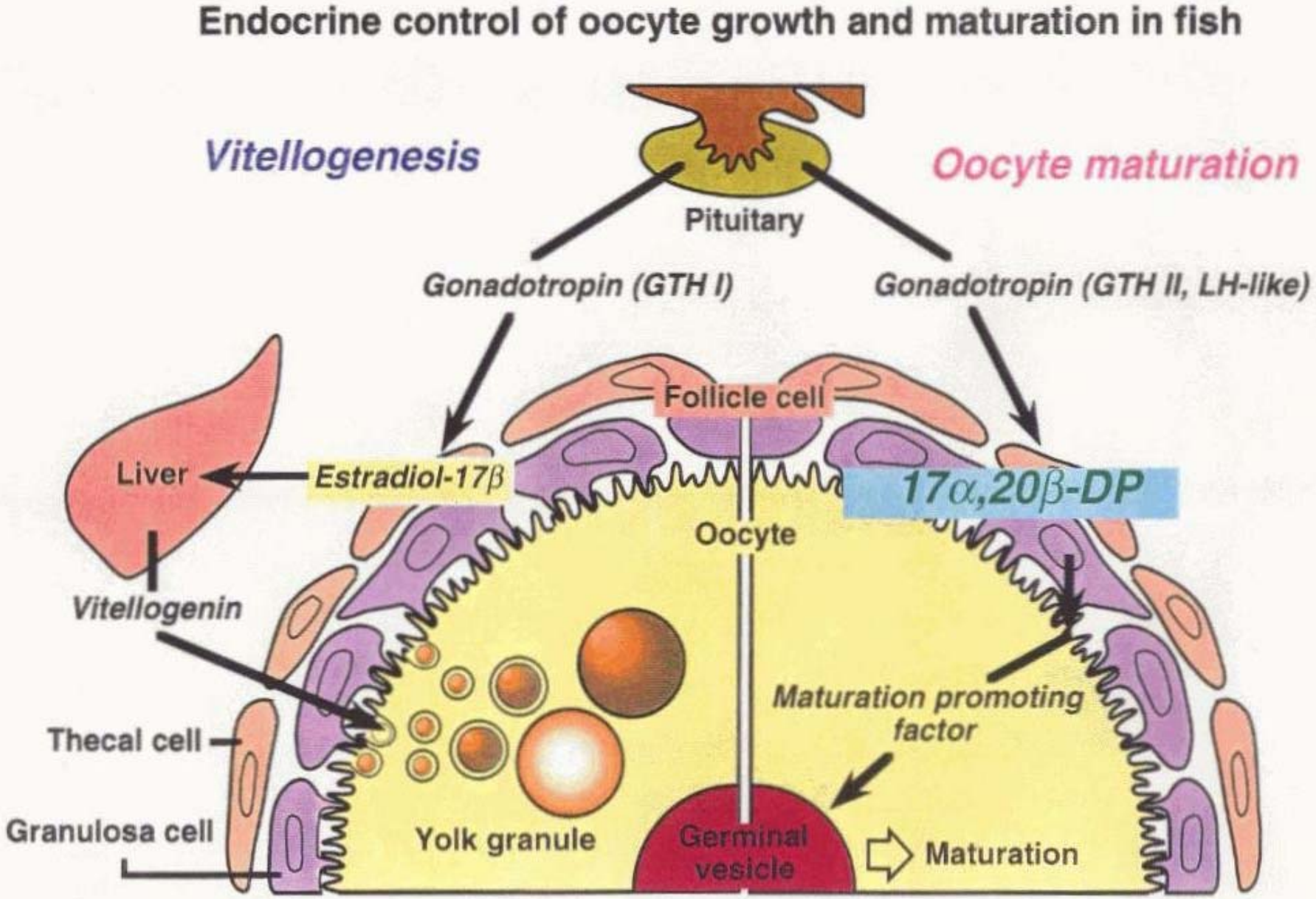
Endocrine control of oocyte growth and maturation in fish
Vitellogenesis
Oocyte maturation
Pituitary
Gonadotropin (GTH I)
Gonadotropin (GTH II, LH-like)
Follicle cell
Liver
Estradiol-17β
17α,20β-DP
Oocyte
Vitellogenin
Maturation promoting factor
Thecal cell
Granulosa cell
Yolk granule
Germinal vesicle
Maturation

Fig. 1

Fig. 2 Two cell-type model for 17α,20β-dihydroxy-4-pregnen-3-one production in oocyte maturation. In this model, GTH II stimulates the thecal layer to produce 17α-hydroxyprogesterone (17α-HP), and also acts on the granulosa layer to enhance 20β-hydroxysteroid dehydrogenase (20β-HSD) activity and, sebsequently converts 17α-HP to 17α,20β-DP.

Two cell-type model for 17α,20β-dihydroxy-4-pregnen-3-one production in oocyte maturation

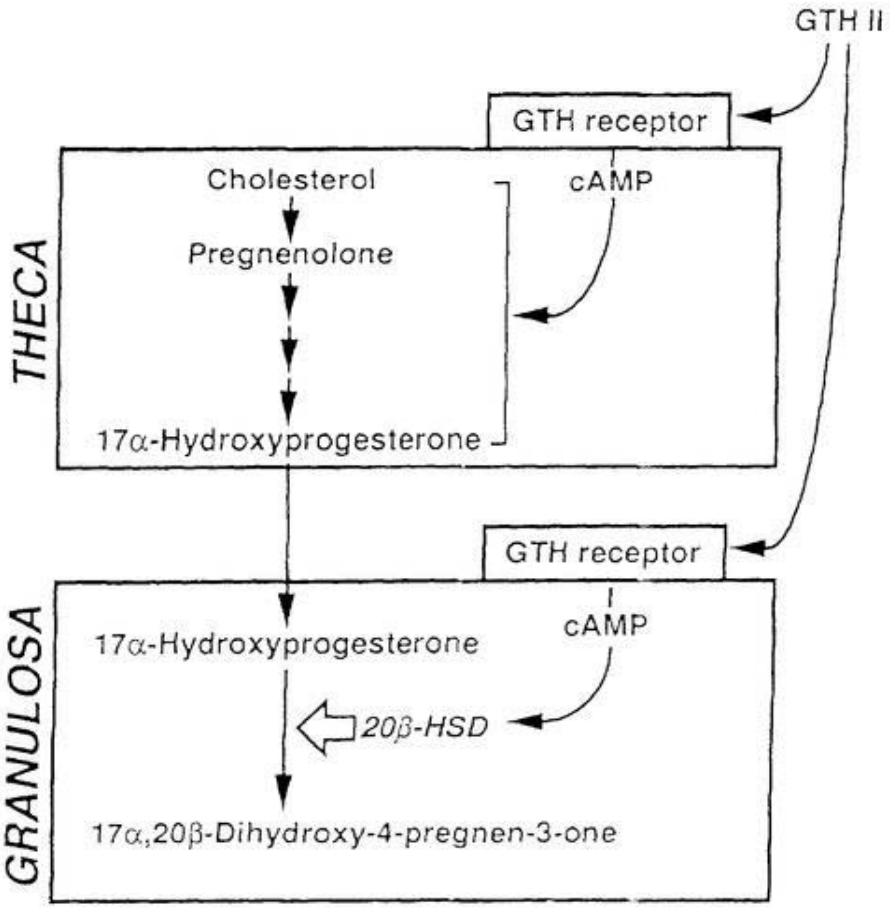


Fig. 2

Fig. 3 Nucleotide sequences of rainbow trout CR/20β-HSD cDNA type A and B. Triangles indicate the places where the introns interrupt the gene. The polyadenylation signal is indicated by a double solid line. Under the third line is the first methionine (Met) of the deduced ORF.

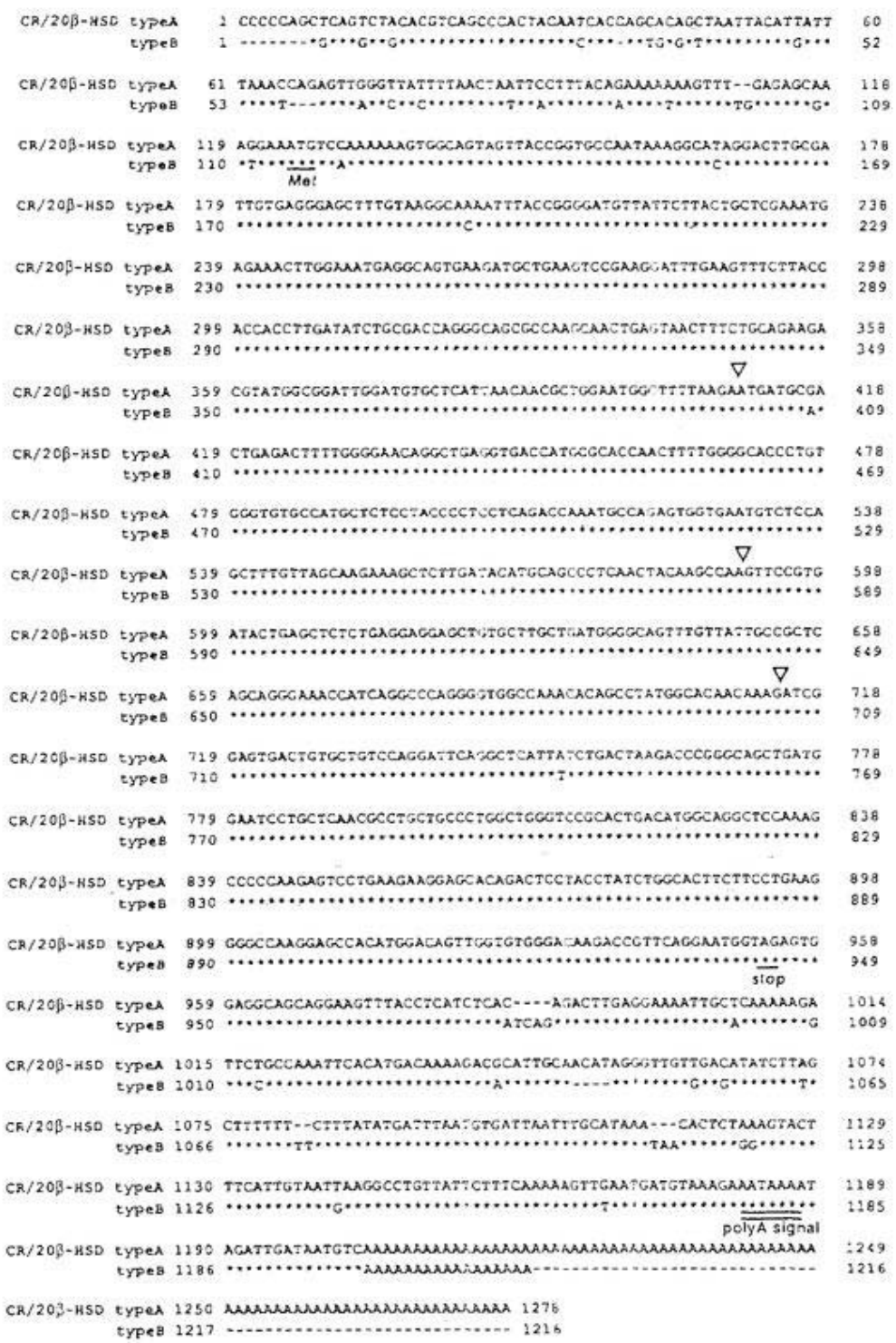


Fig. 3

Fig. 4 Structural organization of rainbow trout CR/20β-HSD genes I and II. The restriction maps of genomic clones are shown above and the locations of the exons are shown below.

CR/20β-HSD gene I

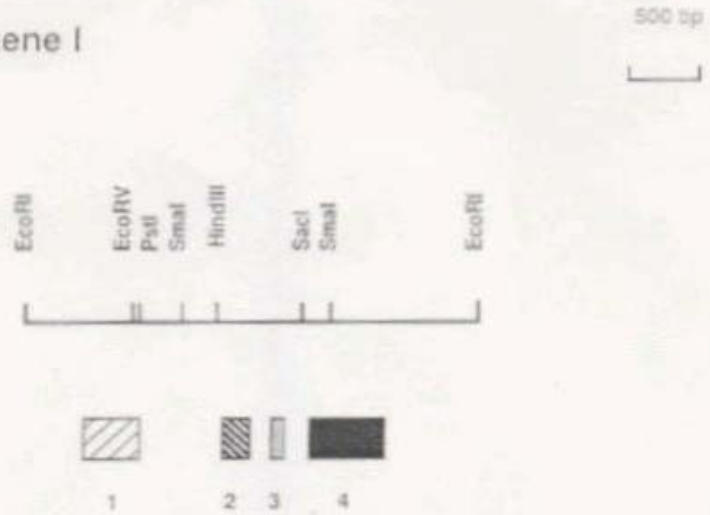


CR/20β-HSD gene II

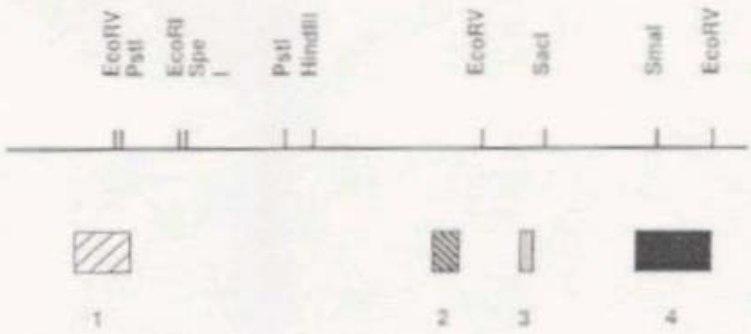


Fig. 4

Fig. 5 Sequence comparison of 5' flanking region of two CR/20β-HSD genes. Sequence site just upstream from cDNA 5'-end is defined as "-1". A putative TATA box at position of -158 and two candidate sites for CRE.1 and Ad4BP are boxed.

## Comparison of 5' upstream regions of CR/20β-HSD type A and B

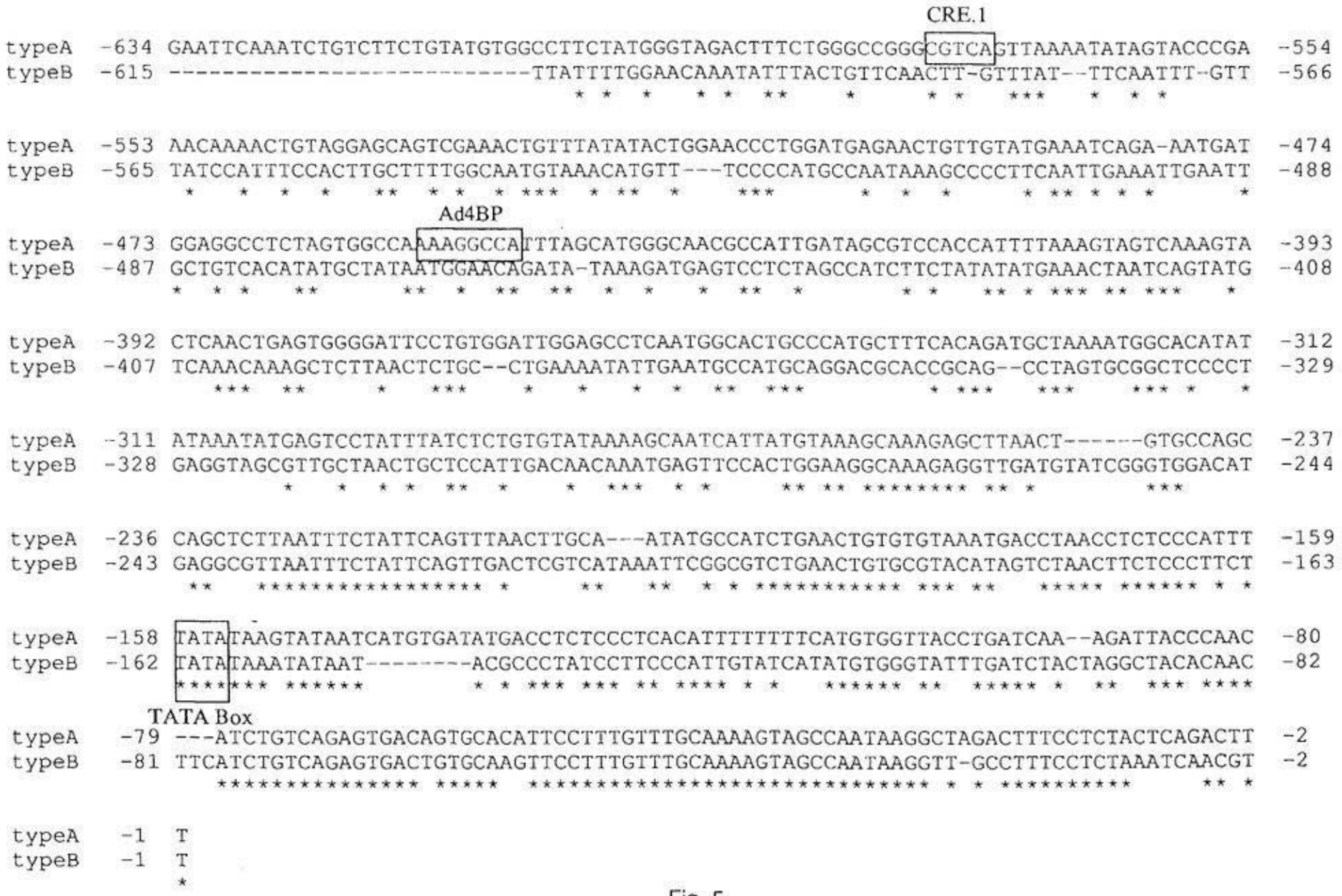


Fig. 5

Fig. 6 Multiple sequence alignment of trout CR/20β-HSDs with mammalian CRs. Sequence alignment of various carbonyl reductases was performed using Mac-Vector soft program (Oxford). Similar residues are boxed and identical residues are shaded. Three sites with distince amino acids (I15, K27 and Y210 in type A) between type A and type B are indicated by '*'.

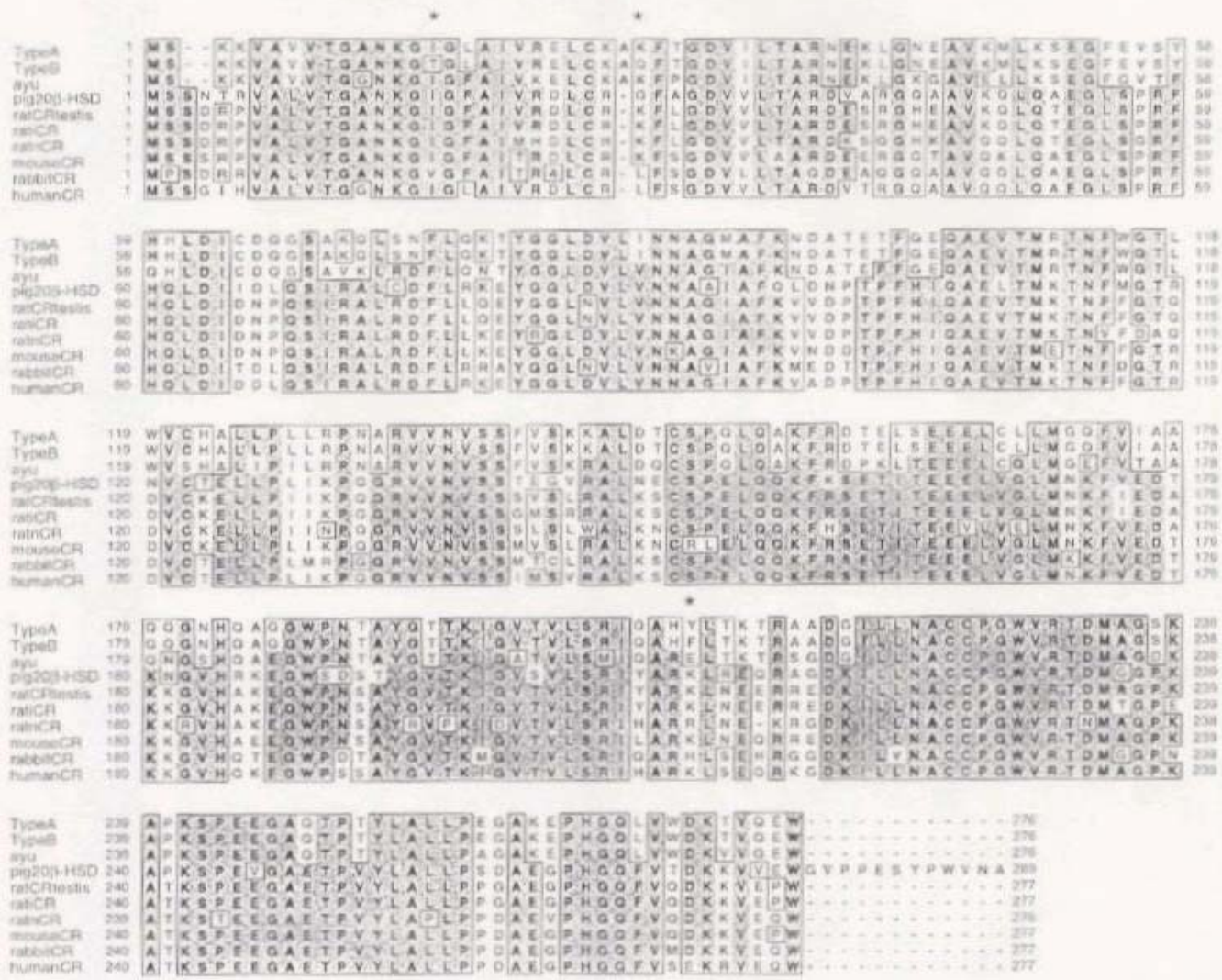
TypeA
TypeB
ayu
pig20β-HSD
ratCRtestis
ratCR
ratnCR
mouseCR
rabbitCR
humanCR

Fig. 6

Fig. 7 20β-HSD activity of recombinant CR/20β-HSD proteins. Open reading frames of CR/20β-HSD cDNA A and B were inserted into the expression vector pET21b+. Expression constructs were transformed into *E. coli*, including pET21b+ as a negative control, and were cultured overnight at 37°C, and then incubated with (IPTG+) or without (IPTG-) for one hour to stimulate protein production. Lysates of cultures were harvested and incubated with [$^3$H]-17α-HP, and steroid products were analyzed by thin layer chromatography. Arrows at the right side indicate the location of authentic 17α,20β-DP and 17α-HP. The arrow in the middle indicates the presence of a band corresponding to [$^3$H]-17α,20β-DP found only when CR/20β-HSD cDNA A was expressed.

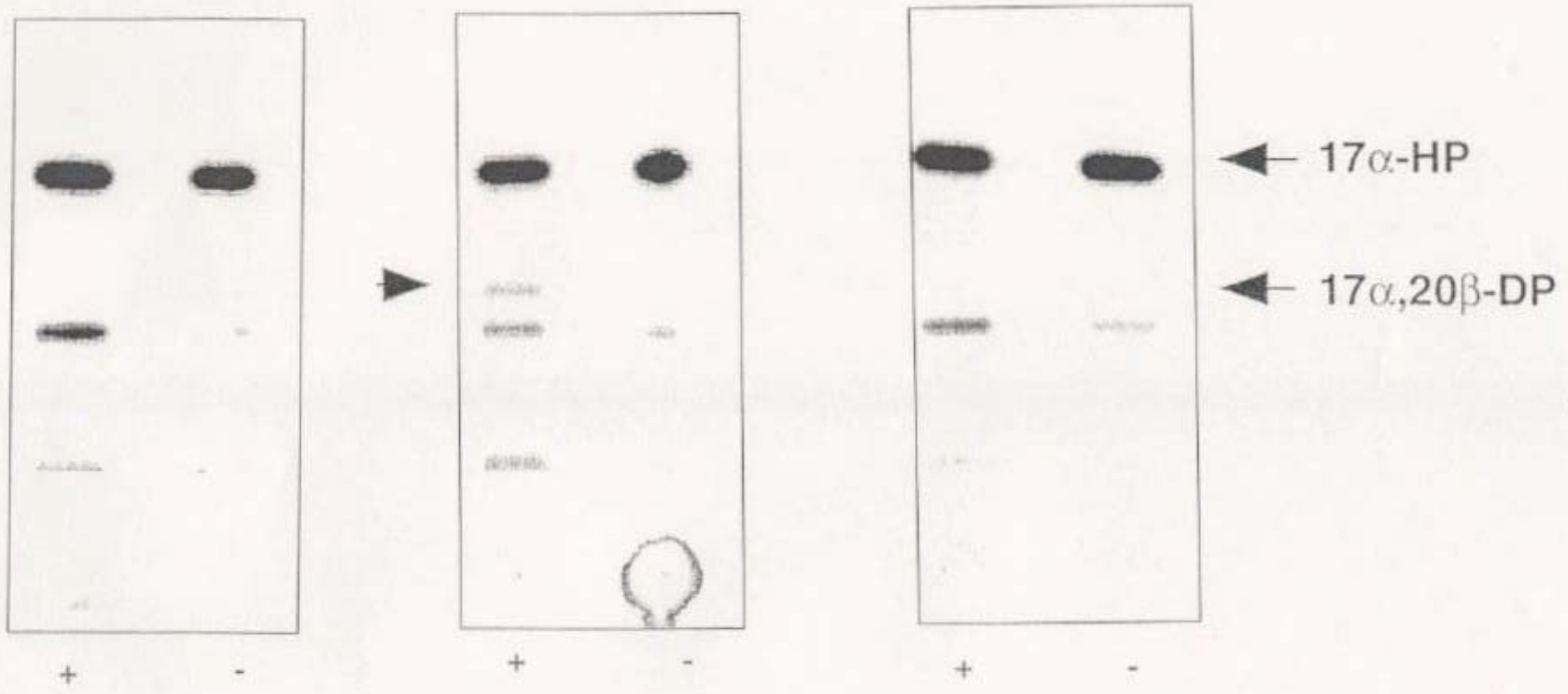


Fig. 7

Fig. 8 Tissue distribution of rainbow trout CR/20β-HSD transcripts. cDNA fragment of CR/20β-HSD type A was used as a probe for detection of tissue distribution of CR/20β-HSD expression (upper panel). β-actin was used as a quantified control (lower panel).

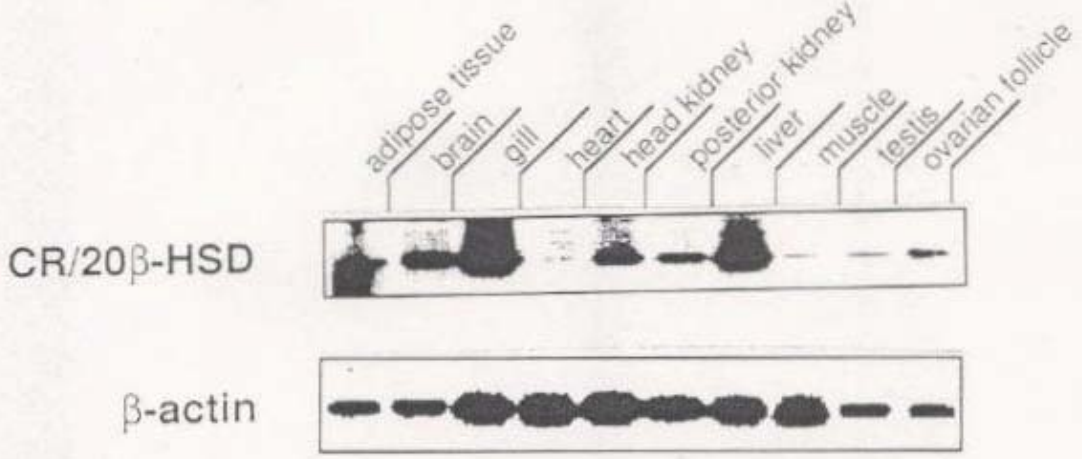
adipose tissue
brain
gill
heart
head kidney
posterior kidney
liver
muscle
testis
ovarian follicle
CR/20β-HSD
β-actin

Fig. 8

Fig. 9 Results of RT-PCR using specific primers for CR/20β-HSD cDNA type A or type B. Fragments amplifed from CR/20β-HSD cDNA type A is shown on upper panel and one from CR/20β-HSD cDNA type B is on lower panel.

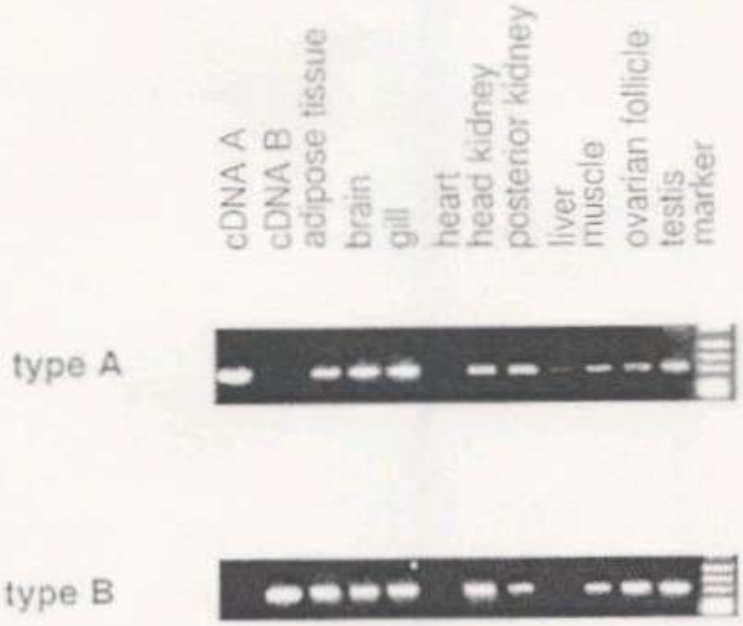
cDNA A
cDNA B
adipose tissue
brain
gill
heart
head kidney
posterior kidney
liver
muscle
ovarian follicle
testis
marker
type A
type B

Fig. 9

Fig. 10 The partial predicted second structures of CR/20β-HSD cDNA type A and type B. The second structure of enzymes were predicted with DNASIS program. α-helix and β-sheet are presented by H(or h) and S(or s). The amino acid residue distinct between type A and type B is indicated by an arrow.

CR/20β-HSD type A


CR/20β-HSD type B

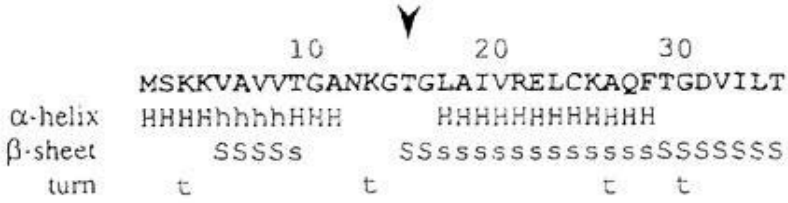


Fig. 10

Fig. 11 The *Nru*I restriction pattern of wild type (type B) and site-directed mutant (B/T15I). The mutagenic oligonucleotide was designed to cointroduce an expected mutation with an *Nru*I site without changing the deduced amino acid. Mutants with an additional *Nru*I stie were isolated using *Nru*I digestion.

Nrul

Marker Mutant Wild type

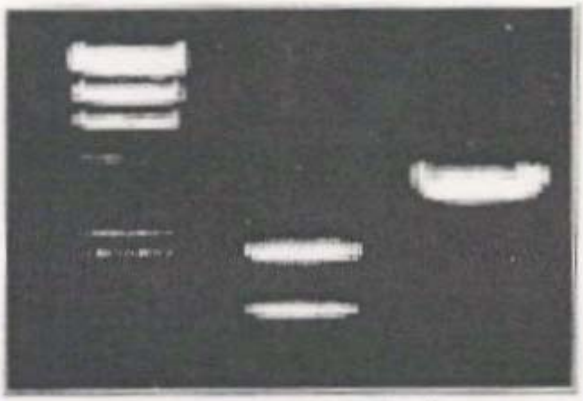

Fig. 11

Fig. 12 Nucleotide sequence of the wild type B and mutant B/T15I. "A" indicated by arrow in type A is replaced by "C" in mutant B/T15I. *Nru*I site is indicated by a single line.

CR/20β-HSD type B

Thr

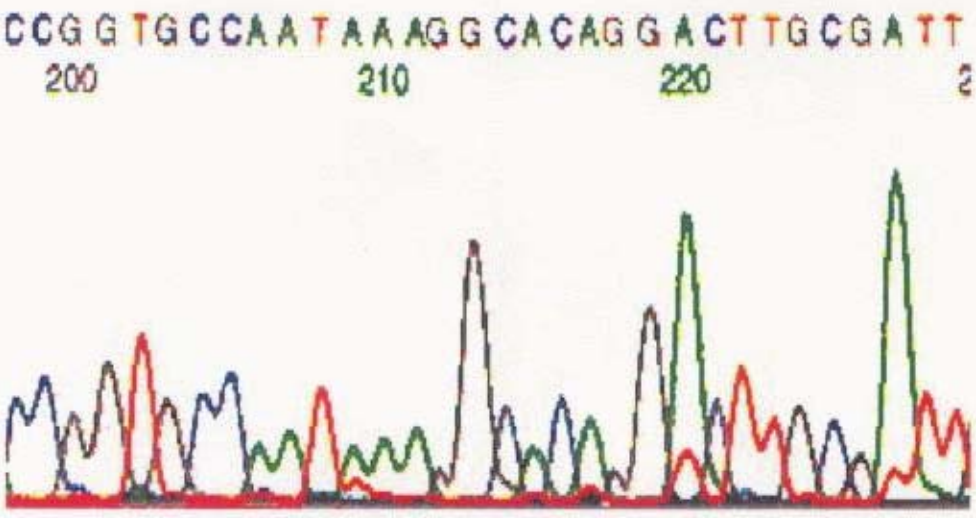


MutB/T15I

Ile

*Nru*I

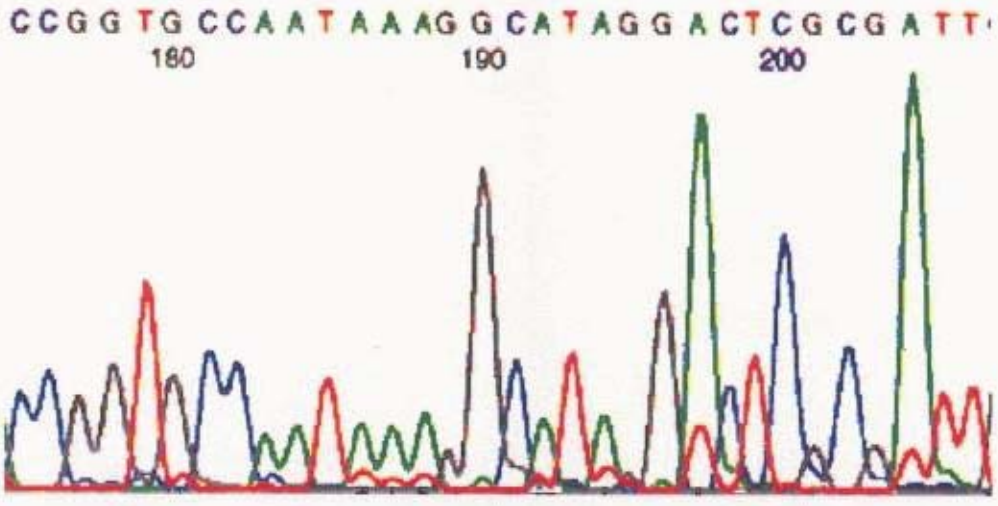


Fig. 12

Fig. 13 Gel electrophoretic patterns of purified recombinants of CR/20β-HSDs and mutants. SDS polyacrylamide gel electrophoresis was performed in 12.5% gels. Proteins were stained with Coomassie Brilliant Blue. The molecular mass (in kDa)of marker proteins is displayed at the left side.


Fig. 13

Fig. 14 Results of thin layer chromatography of wild types as well as mutants incubation with [$^3$H] labeled 17α-hydroxyprogesterone. Arrow indicates the products from incubation with either pET21b+rcA or pET21b+rcB/T15I which were comigrated with standard 17α,20β-DP.

Fig. 15 Fluorescence emission spectra of wild type CR/20β-HSDs and mutants. Spectra of enzymes in 20mM Tris-HCl, 1 mM EDTA buffer (pH 8.0) at an excitation wavelength of 280 nm. Twenty μg of wild type proteins as well as mutants were used and the fluorescence emission were detected via a titration of NADPH (0-2.4 μM). (a) Spectra pattern of wild type A; (b) mutant A/I15T; (c) wild type B; (d) mutant B/T15I. Concentration of NADPH is displayed as A: 0 μM; B: 0.4 μM; C: 0.8 μM; D: 1.6 μM; E: 2.4 μM.

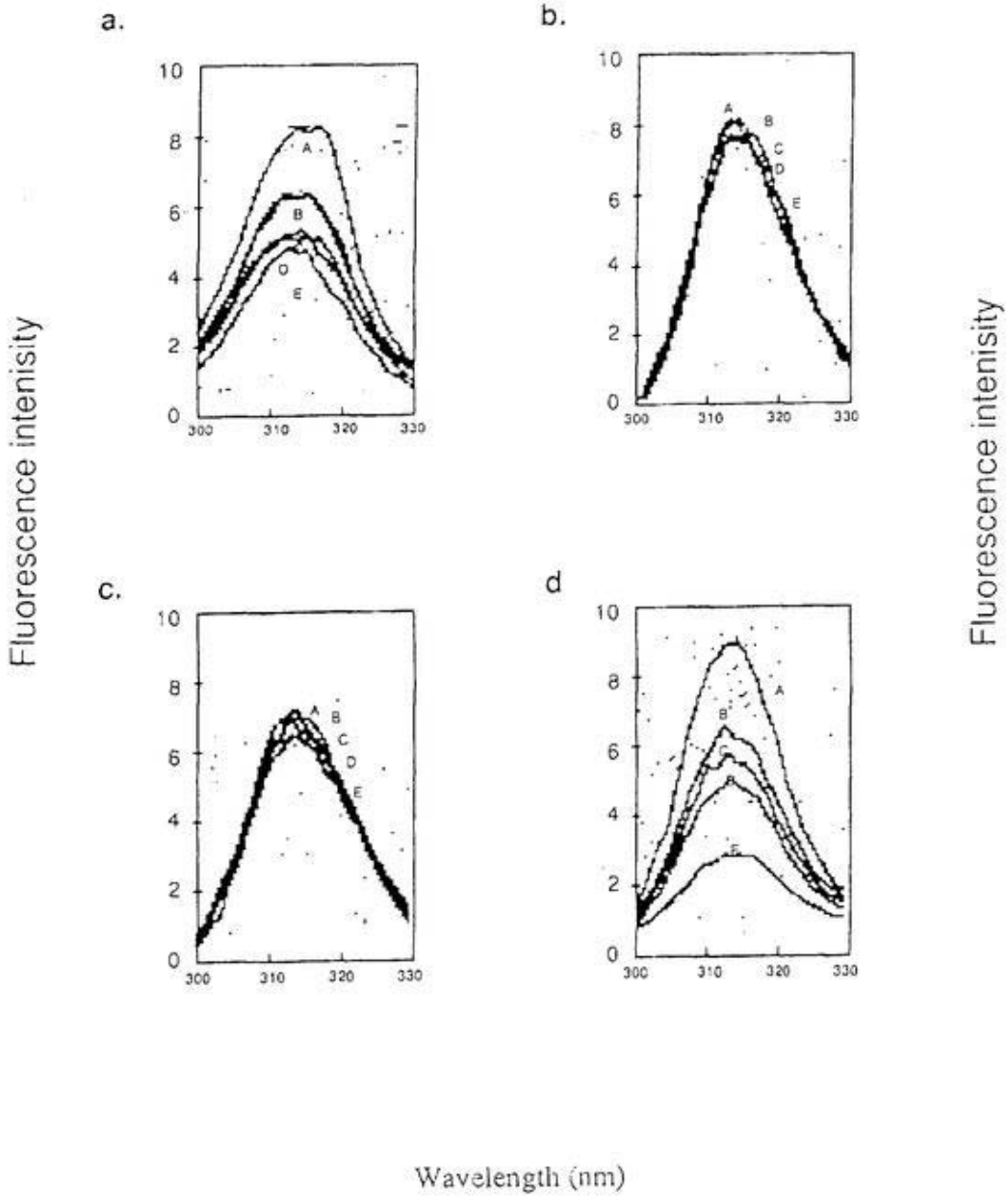
a.
b.
c.
d
Fluorescence intenisity
Fluorescence intenisity
Wavelength (nm)
A
B
C
D
E

Fig. 15

Fig. 16 Steroidogenic pathway in teleost ovary. Two major steroidal mediators in ovarian follicles are produced from cholesterol via a series of derivatives. It is dependent on a cascade of steroidogenic enzymes, whereas *P-450* aromatase and 20β-hydroxysteroid dehydrogenase play an important role in the final production of estradiol-17β and 17α,20β-dihydroxy-4-pregnen-3-one respectively.

Steroidogenic pathway in teleost gonads

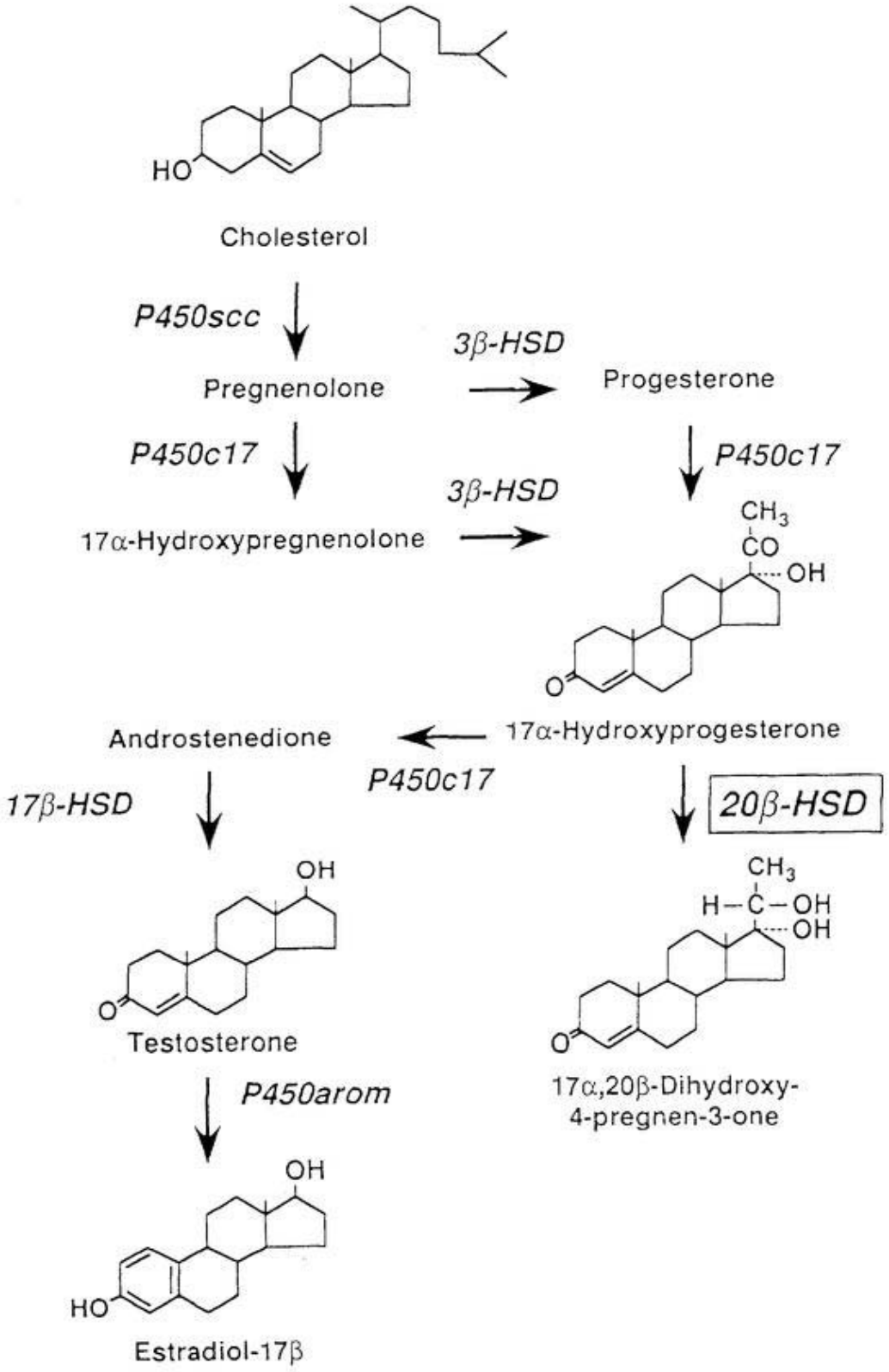


Fig. 16

Fig. 17 Results of Northern analysis of various steroidogenic enzymes during ovarian development. mRNA were extracted from vitellogenic, postvitellogenic, maturing follicles and postovulatory ovary were electrophoresed in a denaturing formaldehyde-agarose gel (1.5%) and transferred onto a nylon membrane. The expression of steroidogenic enzymes was detected by hybridization of membrane with each enzyme's cDNA fragments. Trout β-actin was used as a control for mRNA contents applied in each lane.

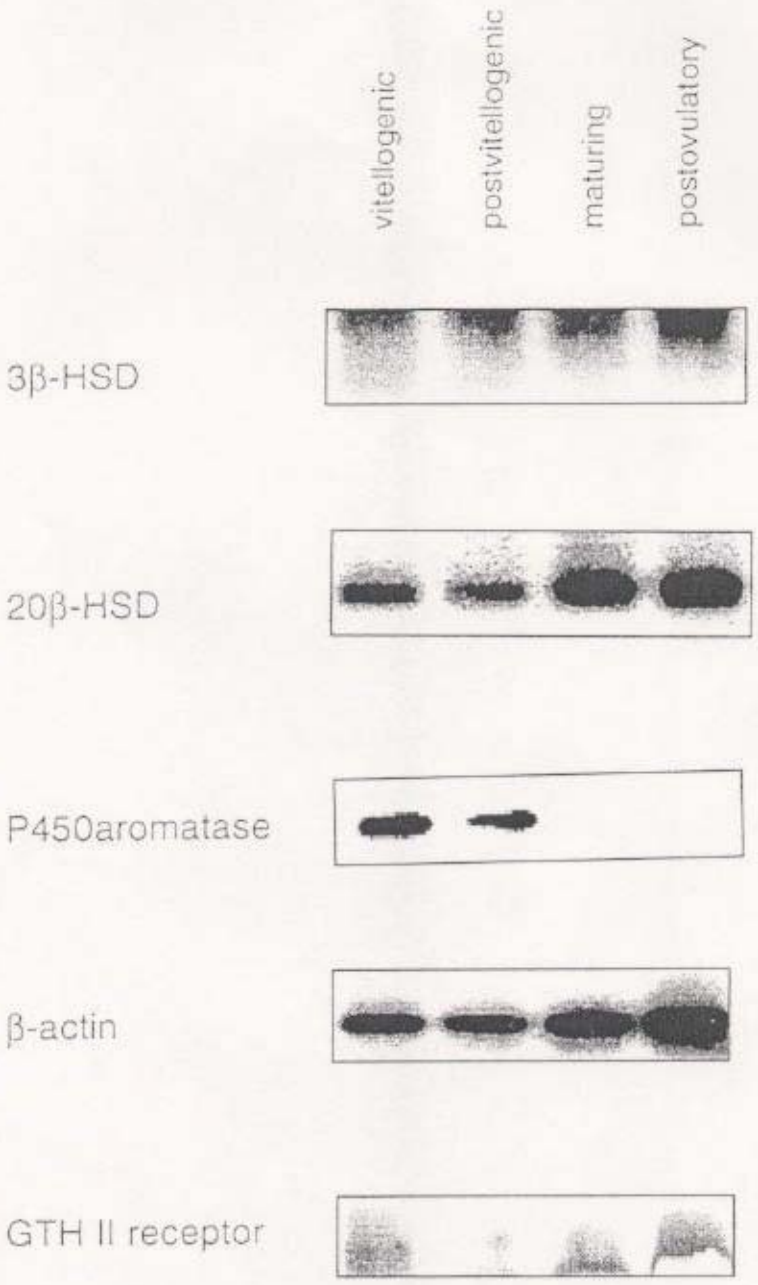
vitellogenic
postvitellogenic
maturing
postovulatory
3β-HSD
20β-HSD
P450aromatase
β-actin
GTH II receptor

Fig. 17

Fig. 18 A comparison of mRNAs of steroidogenic enzymes and maturation-inducing hormone (MIH) production in rainbow trout oogenesis. Expression of 20β-HSD, 3β-HSD, GTH II-receptor and P450arom mRNAs was normalized by β-actin and the quantified P450arom in active vitellogenis stage is defined as 100%.

*Dynamic association of mRNAs of steroidogenic enzymes in ovarian follicle during reproductive development*

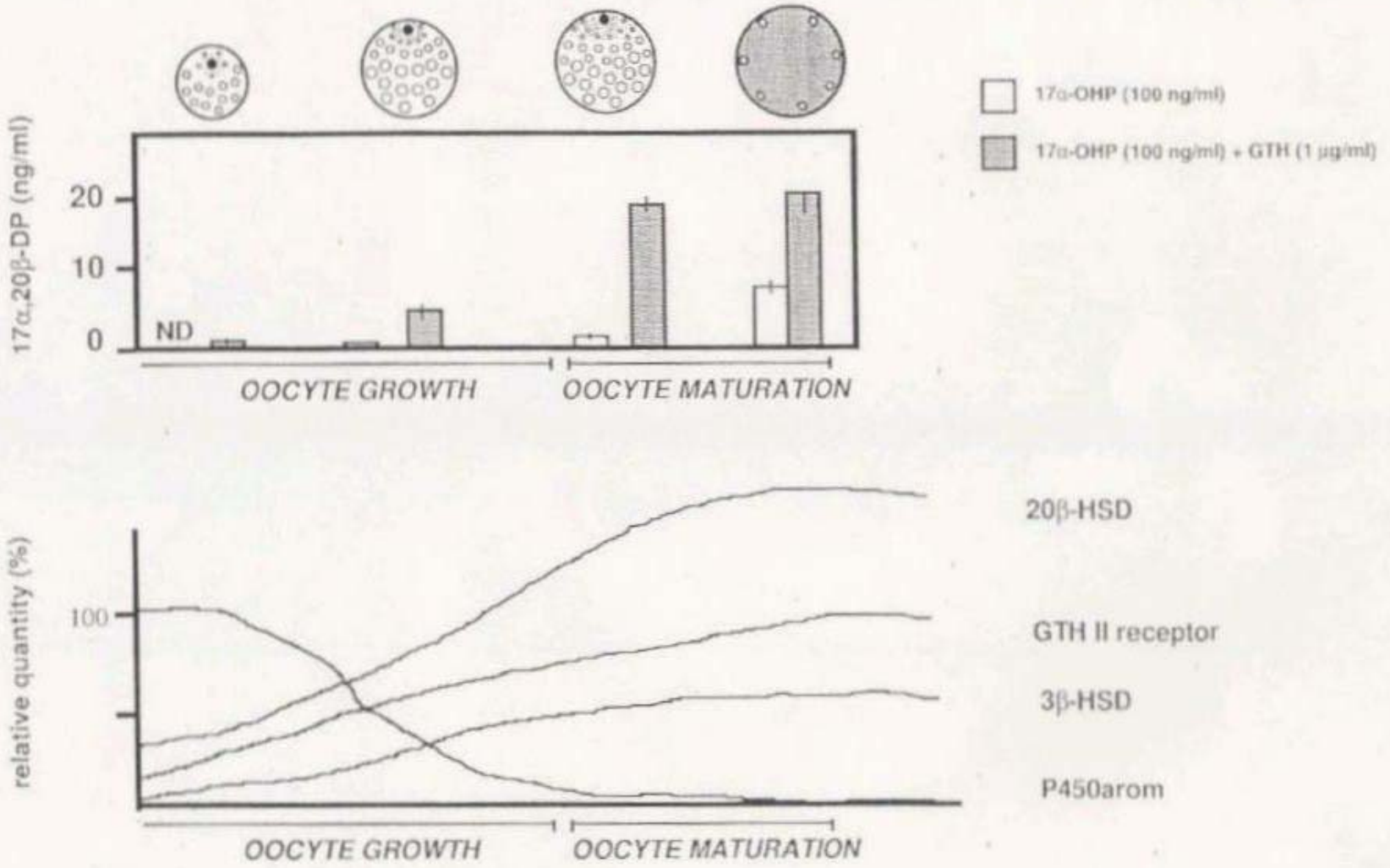


Fig. 18

Fig. 19 Results of radioimmunoassay of 17α,20β-DP production by isolated granulosa cells *in vitro*. The isolated granulosa layers were added in Ringer containing 17α-HP (0.1 μg/ml) and SGA (1 μg/ml) and incubated at 15°C for 12 hours (left panel) or 20 hours (right panel). Results from incubations with 17α-HP are displayed in blank bar, whereas those from incubation with 17α-HP and SGA are in black bar.

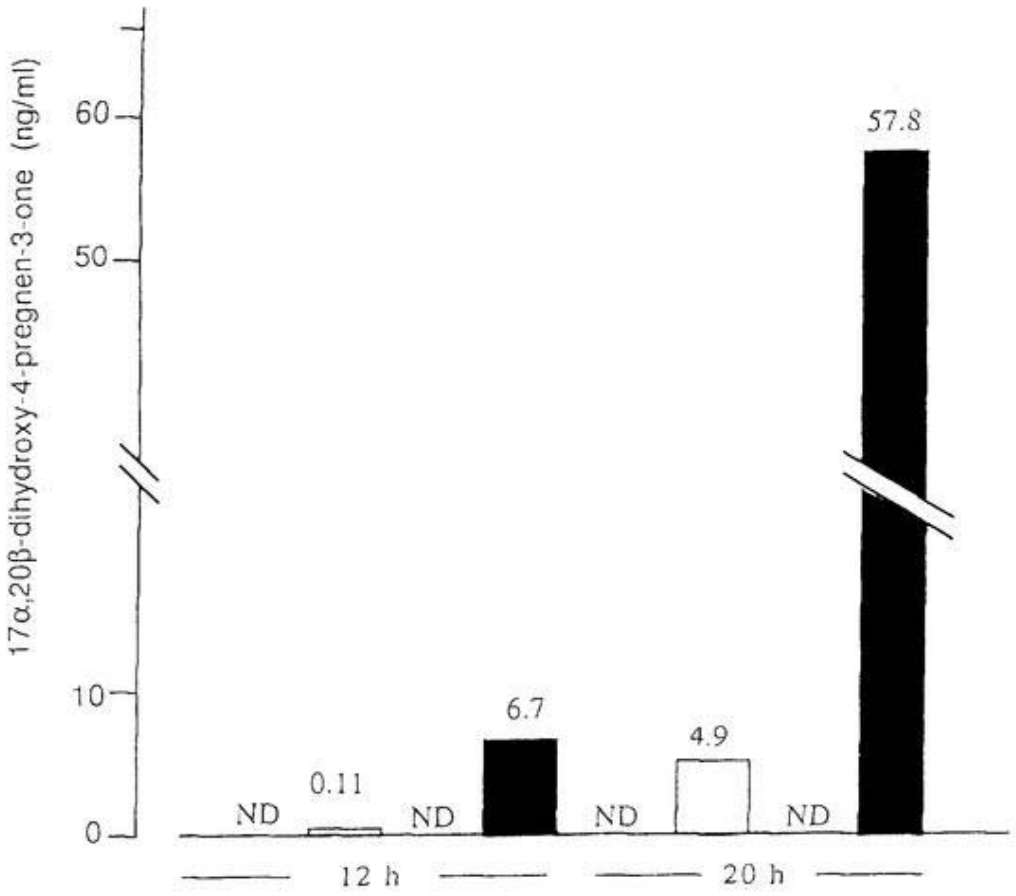


| | | | | | | | | |
|---|---|---|---|---|---|---|---|---|
| 17α-HP (0.1 μg/ml) | - | + | - | + | - | + | - | + |
| SGA (1 μg/ml) | - | - | + | + | - | - | + | + |

Fig. 19

Fig. 20 Northern analysis of granulosa cells incubated with or without GTH. mRNAs from granulosa cells incubated without (0 hour) and with GTH (12 hours, 20 hours) were electrophoresed and transferred onto a nylon membrane. Fragments of 20β-HSD, 3β-HSD and β-actin cDNAs were used as probes for detection of each gene expression.

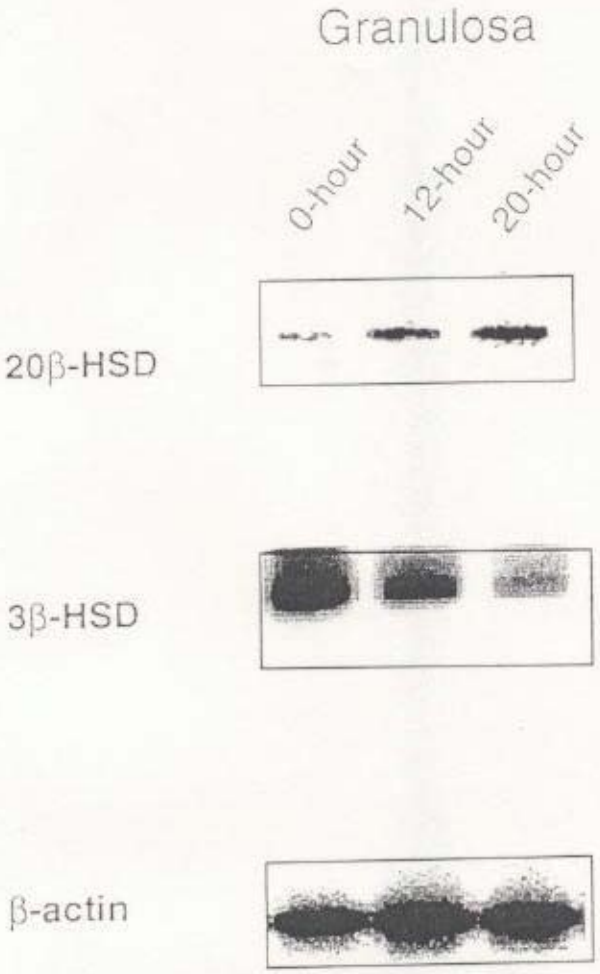


Fig. 20

Fig. 21 RT-PCR results of GTH stimulation CR/20β-HSD expression in granulosa cells. Total RNAs extracted from granulosa cells of 0 hour or incubation with GTH (1 μg/ml) for 20 hours were reversely transcribed and PCR amplified products were electrophoresed in 1.5% agarose gel. Primer sets specific for CR/20β-HSD type A, type B and trout β-actin were used for PCR amplification.

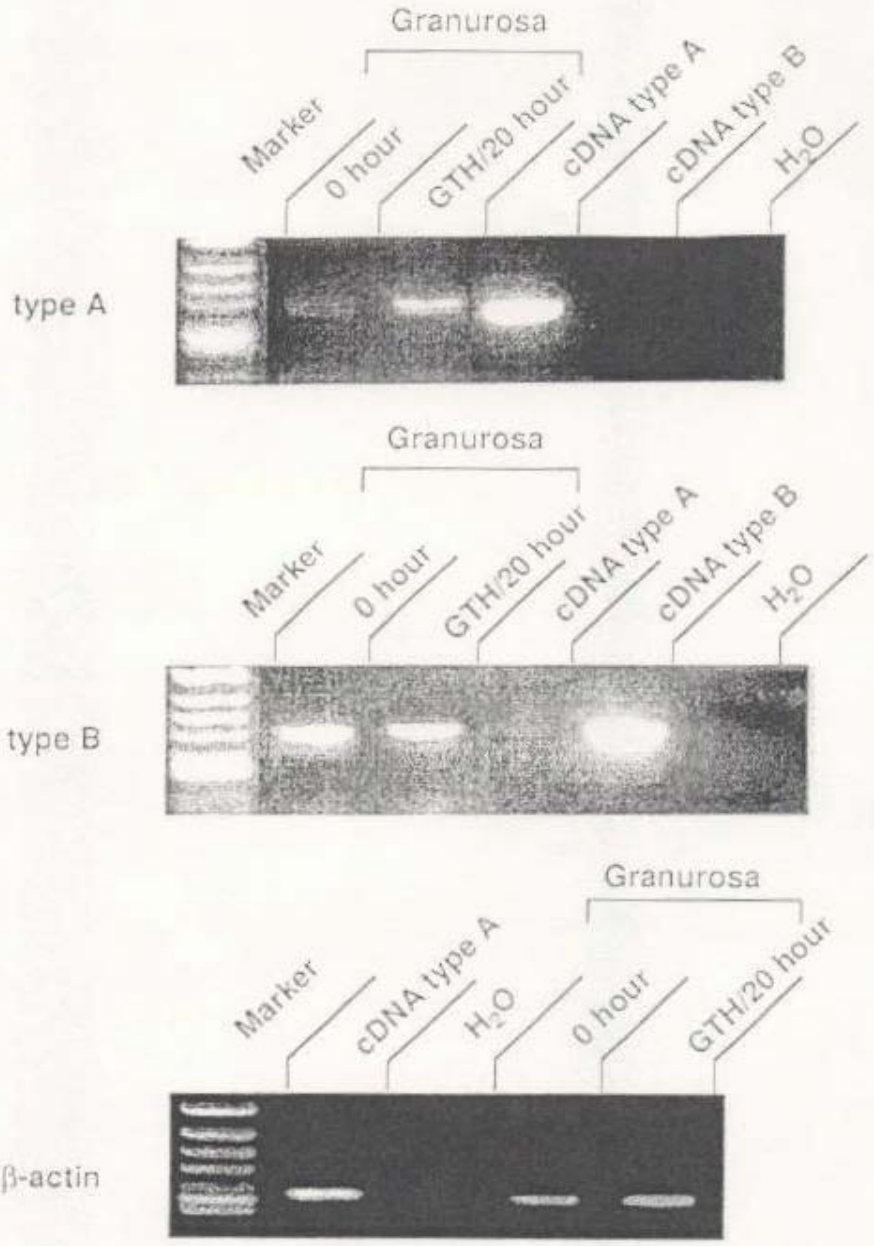
Granurosa
Marker
0 hour
GTH/20 hour
cDNA type A
cDNA type B
H2O
type A
Granurosa
Marker
0 hour
GTH/20 hour
cDNA type A
cDNA type B
H2O
type B
Granurosa
Marker
cDNA type A
H2O
0 hour
GTH/20 hour
β-actin

Fig. 21

Fig. 22 Western blot analysis of CR/20β-HSD. One μg of protein from granulosa cells incubated with Ringer or GTH for 20 hours at 15°C was applied. Left panel shows the result of CBB staining. Middle panel is the result of western blot against anti-tr-3β-HSD-M. Right panel is the result of western blot using anti-CR/20β-HSD.

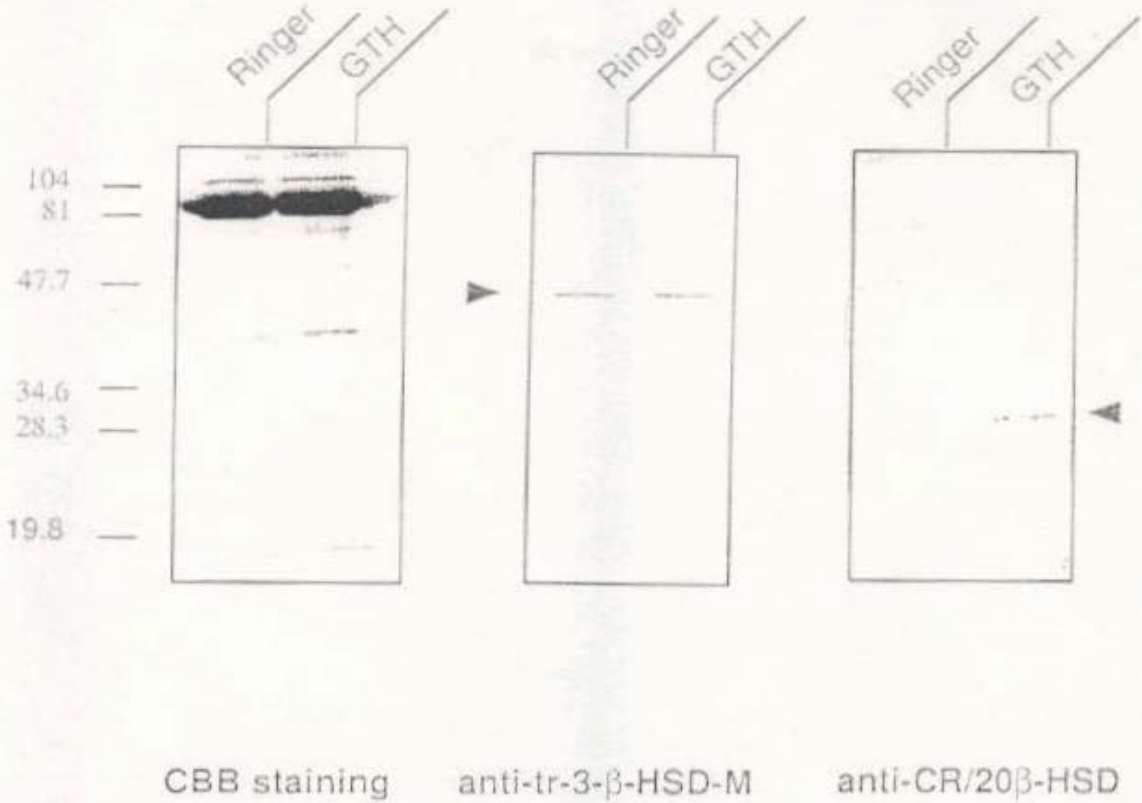
Ringer
GTH
Ringer
GTH
Ringer
GTH
104
81
47.7
34.6
28.3
19.8
CBB staining
anti-tr-3-β-HSD-M
anti-CR/20β-HSD

Fig. 22

Table 1. Exon-intron organization of rainbow trout CR/20β-HSD genes.

| No. | Exon size (base) | Intron size (base) | Sequence of exon-intron junctions | | Similarity between A and B exon/intron |
|---|---|---|---|---|---|
| 1 | 409/401 | 738/2145 | AAGAgttc | .....(t/c)tagATGA | 92%/32% |
| 2 | 181 | 365/349 | CCAAgtat | ..... gaagGTTC | 99%/81% |
| 3 | 123 | 84/1274 | AAAGgtag | ..... ttagATCG | 100%/6% |
| 4 | 561/493 | | | | 81%/--- |

Nucleotide sequences of exons are in capital letters, while those of introns are in lower letters. Sequence differences between genes I and II are indicated by a slash (gene I and gene II), and similarity index is presented by exon/intron.

Table 2. Specific activities of recrystallization

| Specific actiivties of recrystallization (cpm/mg) | | | |
|---|---|---|---|
| 1st | 2nd | 3rd | before crystallization |
| 2309.6 | 2229.8 | 2155.1 | 2910.6 |

Table 3. Comparison of substrate specificity of rainbow trout CR/20β-HSD type A with pig 20β-HSD and human carbonyl reductase.

| Substrate | Conc. mM | Relative velocity (%) | | |
|---|---|---|---|---|
| | | Pig | Human | Rainbow trout |
| 4-Nitrobenzaldehyde | 0.5 | 100 | 100 | 100 |
| Menadione | 0.25 | 62 | 350 | 44 |
| PGE2 | 1 | 0 | 10 | 1.2 |
| 5α-Dihydrotestosterone | 0.05 | 90 | 11 | 23 |
| 5β-Dihydrotestosterone | 0.05 | 29 | 12 | 30 |
| Progesterone | 0.02 | 10 | ND* | 0 |
| 17α-Hydroxyprogesterone | 0.02 | 10 | ND* | 1.2 |

ND*: not detect.

Table 4. Kinetic parameters of recombinants of wild type and mutants of CR/20β-HSD

| | | | NADPH (0.08 mM) | | | NADH (0.08 mM) | | |
|---|---|---|---|---|---|---|---|---|
| Enzyme | Volume | Total protein | Rate | Total activity | Specific activity | Rate | Total activity | Specific activity |
| | µl | µg | 1/min | nmol/min | µmol/min/mg | 1/min | nmol/min | µmol/min/mg |
| wild type A | 100 | 3.54 | 0.0076 | 1.23 | 347 | | ND | |
| wild type B | 500 | 3.54 | 0.0016 | 0.26 | 73.4 | | ND | |
| MutA/I15T | 500 | 3.57 | 0.0012 | 0.19 | 53.2 | | ND | |
| MutB/T15I | 50 | 3.58 | 0.009 | 1.45 | 405 | | ND | |

All activity measurements were performed under assay mixture of 0.5 mM 4-nitrobenzaldehyde in 20 mM Tris-HCl/1 mM EDTA buffer (pH 8.0) at room temperature.

Table 5. NADPH-binding affinity of wild type and mutants of CR/20β-HSD

| Enzymes | NADPH μM | λmax(316) | 1/[NADPH] | 1/ΔF | {1/ΔF}/{1/[NADPH]} | Kd |
|---|---|---|---|---|---|---|
| wild type A | 0 | 7.78 | | | | |
| | 0.8 | 6.05 | 1.25 | 0.58 | 0.46 | 0.54 |
| | 1.6 | 4.55 | 0.63 | 0.31 | 0.49 | |
| | 2.4 | 4.25 | 0.42 | 0.28 | 0.67 | |
| wild type B | 0 | 7.03 | | | | |
| | 0.8 | 6.85 | 1.25 | 5.56 | 4.45 | 4.87 |
| | 1.6 | 6.79 | 0.625 | 4.17 | 6.67 | |
| | 2.4 | 6.35 | 0.42 | 1.47 | 3.50 | |
| MutA/I15T | 0 | 8.25 | | | | |
| | 0.8 | 8.07 | 1.25 | 5.56 | 4.45 | 6.55 |
| | 1.6 | 8.00 | 0.63 | 4.00 | 6.40 | |
| | 2.4 | 7.98 | 0.42 | 3.70 | 8.80 | |
| MutB/T15I | 0 | 8.70 | | | | |
| | 0.8 | 6.83 | 1.25 | 0.53 | 0.42 | 0.53 |
| | 1.6 | 5.70 | 0.63 | 0.30 | 0.48 | |
| | 2.4 | 5.05 | 0.42 | 0.29 | 0.69 | |